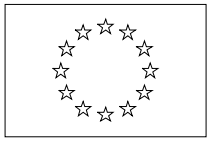

EUROPEAN COMMISSION
5th EURATOM FRAMEWORK PROGRAMME 1998-2002
KEY ACTION : NUCLEAR FISSION

FLOMIX-R
FLUID MIXING AND FLOW DISTRIBUTION IN THE PRIMARY CIRCUIT

Final Summary report
(synthesized version)

CO-ORDINATOR
Dr. Ulrich Rohde
Forschungszentrum Rossendorf Inc.
P.O.Box 51 01 19
D – 01314 Dresden
GERMANY
Tel.: +49 351 260 3460
Fax: +49 351 260 2383

LIST OF PARTNERS
1. Forschungszentrum Rossendorf, Dresden, Germany
2. Vattenfall Utveckling, Älvkarleby, Sweden
3. SERCO ASSURANCE, Warrington, United Kingdom
4. Gesellschaft für Anlagen- und Reaktorsicherheit, Garching, Germany
5. Fortum Nuclear sServices, Espoo, Finland
6. Paul Scherrer Institute, Villigen, Switzerland
7. VUJE Trnava, Slovak Republic
8. Nuclear research Institute Rez, Czech Republic
9. AEKI Budapest, Hungary
10. NPP Paks, Hungary
11. FSUE EDO Gidropress, Podolsk, Russian Federation (external expert organization)
12. TU Budapest, Hungary (observer)
13. NRG Petten, Netherlands (observer)

CONTRACT **FIKS-CT-2001-00197**

Authors

Forschungszentrum Rossendorf (FZR)
U. Rohde, T. Höhne, S. Kliem

Gesellschaft für Anlagen- und Reaktorsicherheit (GRS)
M. Scheuerer

Vattenfall Utveckling
B. Hemström

Fortum Nuclear Services
T. Toppila

Paul Scherrer Institute
T. Dury

VUJE Trnava
J. Klepac, J. Remis

NRI Rez
P. Mühlbauer, L. Vyskocil

AEKI Budapest
I. Farkas

NPP Paks
J. Elter

TU Budapest
A. Aszodi, I. Boros

EDO Gidropress
Y. Bezrukov

Manuscript prepared by

U. Rohde

Contents

Executive Summary

The project was aimed at describing the mixing phenomena relevant for both safety analysis, particularly in steam line break and boron dilution scenarios, and mixing phenomena of interest for economical operation and the structural integrity. Measurement data from a set of mixing experiments, gained by using advanced measurement techniques with enhanced resolution in time and space were used to improve the basic understanding of turbulent mixing and to provide data for Computational Fluid Dynamics (CFD) code validation. Slug mixing tests simulating the start-up of the first main circulation pump have been performed with two 1:5 scaled facilities: The Rossendorf coolant mixing model ROCOM and the VATTENFALL test facility, modelling a German Konvoi type and a Westinghouse type three-loop PWR, respectively. Additional data on slug mixing in a VVER-1000 type reactor gained at a 1:5 scaled metal mock-up at EDO Gidropress are provided. Experimental results on mixing of fluids with density differences obtained at ROCOM and the FORTUM PTS test facility were made available.

Concerning mixing phenomena of interest for operational issues and thermal fatigue, flow distribution data available from commissioning tests (Sizewell-B for PWRs, Loviisa and Paks for VVERs) have been used together with the data from the ROCOM facility as a basis for the flow distribution studies. The test matrix on flow distribution and steady state mixing performed at ROCOM comprises experiments with various combinations of running pumps and various mass flow rates in the working loops.

Computational fluid dynamics calculations have been accomplished for selected experiments with two different CFD codes (CFX-5, FLUENT). Best practice guidelines (BPG) were applied in all CFD work when choosing computational grid, time step, turbulence models, modelling of internal geometry, boundary conditions, numerical schemes and convergence criteria. The BPG contain a set of systematic procedures for quantifying and reducing numerical errors. The knowledge of these numerical errors is a prerequisite for the proper judgement of model errors. The strategy of code validation based on the BPG and a matrix of CFD code validation calculations have been elaborated. Besides of the benchmark cases, additional experiments were calculated by new partners and observers, joining the project later.

Based on the “best practice solutions”, conclusions on the applicability of CFD for turbulent mixing problems in PWR were drawn and recommendations on CFD modelling were given. The high importance of proper grid generation was outlined. In general, second order discretization schemes should be used to minimise numerical diffusion. First order schemes can provide physically wrong results. With optimised “production meshes” reasonable results were obtained, but due to the complex geometry of the flow domains, no fully grid independent solutions were achieved. Therefore, with respect to turbulence models, no final conclusions can be given. However, first order turbulence models like K-ε or SST K-ω are suitable for momentum driven slug mixing. For buoyancy driven mixing (PTS scenarios), Reynolds stress models provided better results.

A. Objectives and Scope

Several various mixing phenomena characterize the various operating conditions of Pressurized Water Reactors (PWR) and influence the safety analyses of the pertaining plant operating states. Turbulent mixing at low flow velocities is governed by the buoyancy forces that are created by the temperature and boron concentration differences. At higher velocities turbulent mixing is governed by the velocity differences of different flow streams. Computational Fluid Dynamics (CFD) is the main tool to study such phenomena. Since there are still large uncertainties in the proper application of turbulence models in various cases, in the suppression of numerical diffusion and in optimum time step selection and mesh size definition, the validation of CFD codes for reactor applications requires well-defined experiments. Such requirements were discussed in a profound manner during the EUBORA Concerted Action focusing on mixing and transport of diluted slugs during boron dilution transients. The conclusion was that it would be beneficial to employ existing 1/5-scale facilities for statistical experiments, combined with the data from the commissioning testing of the plants. The measurement data were used to develop the CFD code capabilities for the determination of the flow distribution to the reactor core and to the different loops as well as for turbulent mixing in the case of slug transport and cold emergency core cooling water.

- The first objective of the project was to obtain complementary and confirmatory data for the resolution of the local boron dilution transients after restart of a RCP. The local boron dilution is considered as potentially leading to a most serious reactivity transient in the PWRs and VVERs. The most important mitigative mechanism is mixing before the slug enters the reactor core. The aim was to carry out experiments in order to understand in sufficient detail, how the slug mixes before it enters the reactor core, and to validate the CFD codes for plant application.

- The second objective was to use the experimental data to justify application of various turbulence and turbulent mixing models for various flow conditions, to suppress numerical diffusion and to decrease grid, time step and user effects in the CFD analyses.

- The third objective was to utilize the experience from the mixing experiments and the plant commissioning test data to justify the application of CFD to determine the primary circuit flow distribution and the effect of thermal mixing phenomena in the context of the structural integrity assessment.

B. Work Programme

The work in the project was performed within five Work Packages.

WP 1: Identification of the key flow mixing and distribution phenomena for the safety analyses and structural integrity applications

Since the aim was to cover mixing phenomena relevant for both safety analysis, particularly in steam line break and boron dilution scenarios, and mixing phenomena of interest for economical operation and the structural integrity, the first work package is focussed on the key phenomenology of various applications. The common features and differences were identified. Test matrices for the experiments and a CFD code validation strategy have been elaborated.

WP2: Slug mixing experiments

Slug mixing experiments were carried out in two existing 1:5-scale facilities of partners FZR and Vattenfall. ROCOM (Rossendorf Coolant Mixing Model) is a test facility modelling a German KONVOI type reactor. The RPV model is made of transparent acryl enabling velocity measurements using LDA techniques. ROCOM is equipped with one fully controllable pump in each of the four loops giving the possibility to perform tests in a wide range of flow conditions. The VATTENFALL facility is a mock-up of the Westinghouse PWR at NPP Ringhals. The un-borated water slugs are modelled in both facilities by means of a salt water tracer solution. Conductivity is measured to determine the mixing of the tracer. CFD calculations performed to analyse the scaling of the models have shown, that under forced flow conditions (high Reynolds numbers), the scaling of 1:5 to the prototype meets both physical and economical demands. The experiments were performed in order to complement the existing data base with the following new information:

- statistical experiments, i.e. 5 similar runs in order to reveal the chaotic behaviour of the swirls in the downcomer,
- experiments with emphasis on velocity measurements that are mainly missing,
- effect of scaling, i.e. Reynolds versus Strouhal scaling and Froude scaling.

Improved measurement techniques being capable of providing data on turbulent mixing phenomena with enhanced resolution in time and space have been employed. To investigate the Reynolds versus Strouhal scaling, the height, the slope and the length of the start-up ramps were varied from normal pump start-up conditions down to parameters typical for the start-up of natural circulation. Additional data on slug mixing in a VVER-1000 type reactor gained at a 1:5 scaled metal mock-up at EDO Gidropress have been provided.

Besides of slug mixing data, experimental results on buoyancy driven mixing of fluids with density differences obtained at ROCOM and the FORTUM PTS test facility have been made available. Buoyancy driven mixing is relevant for PTS scenarios. Froude number scaling was considered for experiments with density differences.

WP 3: Flow distribution in the primary circuit

Experiments on the flow distribution in the 4-loop PWR with running RCPs were carried out at ROCOM allowing the operation with different controlled mass flow rates in the various loops. Salt water plugs are injected near the cold leg outlet nozzles. The degree of mixing is determined from conductivity measurements by the help of high resolution wire mesh sensors. Additional test data were made available for the project by Paks NPP, based on the commissioning tests, typical for VVER conditions. The tests performed at the plant addressed mixing among coolant loop flows in the downcomer and up to the core inlet in forced flow conditions. For that purpose one or more loops were running at temperatures different from that of the other loops and the core outlet temperature distribution was recorded at 212 fuel assemblies out of a total of 349. The test scenario is important for the "classical" VVER-440 design, with typical cold leg and main circulating pump design. There are earlier experiments aimed for determination of the mixing factors for VVER-440 reactors, too. These experiments were performed at zero reactor power in Loviisa VVER-440 NPP.

Computational Fluid Dynamics (CFD) methods were used for the simulation of the flow field in the primary circuit of the operating reactors. Computed results were compared to available measurement data, and conclusions were drawn concerning the usability and modelling requirements of CFD methods for that kind of application.

WP 4: Validation of CFD codes based on the mixing experiments

The experimental results from the mixing experiments were used to evaluate the quality and trust of different CFD modelling approaches for reactor applications. The objectives were to

- examine the effect of mesh size, time step, boundary conditions and detail in description of geometry,
- define appropriate numerical schemes which allow to reproduce physically real solutions and show appropriate convergence behaviour,
- examine the applicability of different turbulence models for a number of different fluid mixing and flow distribution situations.

A limited set of benchmark tests for CFD code validation was derived from the experiments. The ERCOFTAC and ECORA “Best Practice Guidelines” are referenced [BPG, Men02]. Systematic studies concerning numerical errors and model errors have been performed according to the BPG. Efforts were made to calculate steady-state mixing and flow distribution, slug mixing tests and buoyancy induced mixing cases. The codes used were CFX and FLUENT, which allow accurate and flexible modelling of geometry and inclusion of various physical models. The experience from the applications was compiled in a final report and will be used as recommendations for using CFD to different mixing cases.

WP 5: Evaluation of the results, reporting and co-ordination

Information on the status of experimental and CFD code applications has been collected and compared from the various Work Packages. The main results of the project are:

- an unique experimental data base on steady state flow distribution, slug mixing and

buoyancy driven mixing with enhanced resolution in time and space gained from test facilities representing various European reactor types,
- conclusions on flow distribution and temperature fluctuations in NPPs under normal operation conditions being important for economical operation and the estimation of thermal fatigue,
- the recommendations for the CFD applications concerning applied turbulence modelling features, concerning geometrical modelling, meshing and time step, numerical solution schemes, and turbulence modelling features.

The final reports on the work packages 2 (slug mixing), 3 (flow distribution) and 4 (CFD code validation) are public to support the dissemination of the results of the project [1], [2], [3]. An overview on the experimental data base gained within FLOMIX-R is given in [4]. A general overview of the project is provided on the FLOMIX-R web page http://www.fz-rossendorf.de/FWS/FLOMIX/ .

C Work performed and results

C.1 Identification of the key mixing phenomena (WP 1)

The identification of the key phenomena is elaborated in [5], mainly based on the final report of the EUBORA Concerted Action on boron dilution [6]. The objectives of WP1 were:

- identification of the key phenomena important for slug mixing (forced and buoyancy induced),
- identification of the key phenomena important for overcooling transients and normal operation conditions,
- planning of work to be performed for CFD code validation,
- elaboration of the test matrix for the slug mixing experiments.

The main objective of the investigations was to understand in sufficient detail, how water of different quality mixes in the cold leg and in the downcomer of a PWR before it enters the reactor core. These different quality might be different temperatures, different densities and/or different concentrations of additives. The most relevant additive to the primary coolant in PWR is boron acid used for the control of reactivity. In some cases, dependent on the scenario of the transient, both temperature and boron acid concentration might be different in the slug mixed with ambient water, in some cases density differences due to temperature gradients can be neglected with respect to mixing.

The mixing of lower borated slugs with water of higher boron concentration is the most mitigative mechanism against serious reactivity accidents in local boron dilution transients, and therefore, is one of the most important, nuclear safety related issues of mixing. Significant advantage in boron dilution transient analysis can be achieved, if realistic mixing data are used [7], [8].

Local or heterogeneous boron dilution refers to all events that could lead to formation of partially diluted or completely un-borated slugs in the primary system. In the FLOMIX-R project, emphasis was put on heterogeneous dilution considering the transport and turbulent

dispersion of a slug of lower borated water which might be formed in the primary circuit by various mechanisms.
Lower borated slugs can be formed in the primary circuit of a PWR due to external or inherent boron dilution events. An external dilution refers to the cases where diluted or pure water slug is created by injection from outside of the primary circuit. Examples of such are an eventual injection of un-borated coolant or coolant of reduced boric acid concentration by the makeup system, and injection of un-borated pump sealing water to the primary system. Steam generators, chemical and volume control system, diluted accumulator or diluted re-fueling water storage tank and diluted containment sump are mentioned as potential sources of diluted water. Dilution may occur during power operation, shutdown or accident conditions. The sequence of events may vary significantly in different scenarios: pure water from the secondary side may flow to the primary circuit due to maintenance errors during shutdown, reactor coolant pumps (RCP) may stop during inadvertent dilution thus initiating slug formation or inadvertently diluted accumulators may leak to primary circuit during power operation or during accident conditions. An inherent dilution mechanism is connected with the formation of slugs of under-borated water through an inherent phenomenon during an accident. Such an inherent phenomenon can be a boiling-condensing heat transfer mode occurring inside the primary system, or back flow from the secondary system in case of primary-to-secondary leakage accidents.

In VVER-440 reactors, because of the complex geometry of the primary loops and the main gates valves in both the hot and cold legs, there are various extra aspects of slug formation and transport. Particularly, main gate valves in VVER-440 can be closed during reactor operation to isolate single loops for maintenance. The water in these isolated loops might be under-borated due to failure of the water make-up system. The nuclear consequences of transients after re-start of an isolated loop in a VVER-440 type reactor have been studied in [9].

The mixing of slugs of water of different quality is also very important for pre-stressed thermal shock (PTS) situations. In emergency core cooling (ECC) situations after a LOCA, cold ECC water is injected into the hot water in the cold leg and downcomer. Due to the large temperature differences, thermal shocks are induced at the RPV wall. Temperature distributions near the wall and temperature gradients in time are important to be known for the assessment of thermal stresses. One of the important phenomena in connection with PTS is thermal stratification, a flow condition with a vertical temperature profile in a horizontal pipe. The fluid is in single-phase regime unlike in case when the upper part of the pipe is filled with steam, which is not elaborated within this context. Typically a stratified condition builds up, when a low-velocity cold fluid enters to a low-velocity warm fluid in a horizontal pipe. Stable stratification is not particularly dangerous for the pipe itself in structural integrity sense. However, in a real process there are often disturbances that make the temperature boundary to move vertically. Velocity difference between the colder and warmer fluids may also cause wave formation in the temperature boundary. All this may cause thermal fatigue in the pipe. Besides of thermal fatigue, a single thermal shock can also be relevant for structural integrity, if it is large enough, especially in the case, that the brittle fracture temperature of the RPV material is reduced due to radiation embrittlement. Therefore, additional to the investigations of slug mixing during re-start of coolant circulation, the mixing of slugs or streams of water with higher density with the ambient fluid in the RPV were performed. The aim of these investigations was to study the process of turbulent mixing under the influence of buoyancy forces caused by the temperature differences. Heat transfer to the wall and thermal conductivity in the wall material have not been considered.

Another objective of the investigations was to utilize data from steady state mixing experiments and plant commissioning test data to determine the primary circuit flow distribution and the effect of thermal mixing phenomena in the context of the improvement of normal operation conditions and assessment of overcooling transients. Overcooling scenarios are mainly connected with steam line breaks. Inadvertent opening of turbine valves or other valves in the secondary circuit of a NPP are characterized by the same consequences and phenomena. Steam line breaks can be classified by different criteria. A break at full power conditions enhances the heat transfer to the secondary side and leads to the closure of the turbine valves and the reactor trip, inserting a high negative reactivity into the core. The heat release after the trip reduces the amount of overcooling. A break at hot zero power or in the state after a reactor scram is characterised by an increase of the heat transfer to the secondary side from nearly zero to values greater than in the nominal regime of the reactor. The effects of overcooling are higher and are not reduced by a fuel heat release. Depending on the scenario, the reactor coolant pumps can be switched-off or stay in operation during the transient. Running pumps transport the perturbation to the reactor core very quickly. In case of switching-off all RCP, a developed natural circulation establishes after running out of the pumps. A special case is the switching-off the RCP in the broken loop, only. In that case, reverse flow in this loop establishes and the perturbation is not transported to the core directly. A break of one main steam line is characterised by an asymmetric perturbation of the primary circuit. To estimate the impact on the reactor core, the mixing of coolant of different temperature coming from the broken and intact loop has to be assessed. Different from heterogeneous boron dilution events, the change of coolant temperature and the change of flow rates in the individual loops is relatively slow (in comparison to the transport time of the temperature perturbation from the primary circuit cold legs to the core inlet). That's why, the coolant mixing can be considered as quasi-stationary with fixed temperature distribution and mass flow rates at a certain moment of time. Therefore, the mixing can be assessed based on experiments and calculations for steady-state flow situations. Nuclear analysis of main steam line break scenarios based on advanced coolant mixing modelling is reported about in [10].

However, steady-state mixing and flow distribution is not only relevant for overcooling scenarios, but also for nominal operation of the reactor or operational transients. In operational transients, e.g. switching off or switching on single reactor coolant pumps during commissioning tests, the coolant temperature distribution at the core inlet is also non-homogeneous. In these cases, the pressure drop between the lower and the upper plenum of the reactor forces the coolant in the idle loops to flow through the loops in reverse direction. The coolant from the operating and non-operating loops is mixed in the lower and upper plenum of the reactor. Even for nominal operation of the NPP, flow distribution and mixing is important, because mass flow rates and cold leg temperatures of the individual loops can differ by some percent respectively degrees because of differences in the geometry of the loops including steam generators or of pump characteristics. The knowledge of the correct temperature distribution at the core inlet is important for increasing the accuracy of reactor power estimation.

Based on the identification of the key mixing and flow distribution phenomena relevant for both safety analysis, particularly in steam line break and boron dilution scenarios, and for economical operation and the structural integrity, test matrices for the experiments are elaborated. Experiments on slug mixing have been performed at two test facilities, modelling different reactor types in scale 1:5, the Rossendorf and Vattenfall test facilities. The corresponding

accident scenario is the start-up of first RCP after formation of a slug of lower borated water during the reflux-condenser mode phase of a small break LOCA. The measurement data have been made available for CFD code validation purposes. Slug mixing tests have also been performed at the VVER-1000 facility of EDO Gidropress to meet the specifics of this reactor type. Experiments on density driven mixing were carried out at the Rossendorf and the Fortum PTS facilities. The test facilities and selected results of some tests are described in section C.2 of this report.

Concerning steady-state mixing and flow distribution in the cold legs and pressure vessel of the primary circuit, commissioning test measurements performed at the Paks and Loviisa VVER-440 NPPs are used for the estimation of thermal mixing of cooling loop flows in the downcomer and lower plenum of the pressure vessel. A series of quasi steady state mixing experiments are performed at the ROCOM test facility. Description of the experimental results as well as conclusions on flow distribution are presented in section C.3.

Following aspects of mixing not yet fully covered by previous investigations were pointed out in the EUBORA report [6]:

(1) velocity measurements in the downcomer and lower plenum, especially during RCP restart,
(2) Reynolds scaling versus Strouhal scaling,
(3) effects of downcomer geometry and lower plenum structures,
(4) impact of the number and the orientation of primary loops,
(5) transition from buoyancy driven to momentum driven mixing,
(6) full-scale conditions.

In the slug mixing experiments performed within the FLOMIX-R project, mainly the items (1) to (4) have been covered. These aspects were taken into account elaborating the slug mixing test matrix described in section C.2. Additional slug mixing experiments at a mock-up of a VVER-1000 reactor have been provided by EDO Gidropress. These experiments address the effect of geometry and primary loop configuration specific for VVER-1000 reactors, on the one hand, and Reynolds and Strouhal scaling on the other hand.

Considering item (5), the impact of density differences of the mixing fluids has to be considered. To address this aspect, the results of experiments on the generic investigation of the transition between density controlled and momentum driven mixing performed at ROCOM and measurement data from PTS experiments carried out at the Fortum test facility have been made available.

Item (6), concerning full-scale conditions, could not be directly addressed within the project because only scaled test facilities were available. Conclusions on the mixing in real reactor conditions have been gained from measurement data on flow distribution from NPPs. However, no scaled counterpart tests for these measurements are available.

C.2 Slug mixing tests (WP 2)

C.2.1 Description of the test facilities

ROCOM (**Ro**ssendorf **Co**olant **M**ixing Model) is a test facility for the investigation of coolant mixing operated with water at room temperature [11]. The facility models a KONVOI type reactor with all important details for the coolant mixing in a linear scale of 1:5. ROCOM is a four-loop test facility with a RPV mock up made of transparent acryl (Fig. 1). Individually controllable pumps in each loop give the possibility to perform tests in a wide range of flow conditions, from natural circulation to nominal flow rate including flow ramps (pump start up). The transparent material for the pressure vessel allows the measurement of velocity profiles in the downcomer by laser Doppler anemometry.

Both boron concentration and temperature fields are modelled by the concentration field of a tracer solution. The disturbance is created by computer controlled injection of salted water into the cold leg of one of the loops, while the test facility is operated with de-mineralised water. The test facility is equipped with wire-mesh sensors for the electrical conductivity measurement [12], [13] which allow a high resolution determination of the transient tracer concentration in space and time. Four such sensors are installed in the reactor pressure vessel model with altogether about 1000 single measurement positions and a measuring frequency of up to 200 Hz. The location of the sensors in the model is shown on Fig. 2.

The measured conductivity values are transformed into a mixing scalar $\Theta_{x,y,z}(t)$. It is calculated by relating the local instantaneous conductivity $\sigma_{x,y,z}(t)$ to the amplitude of the conductivity change in the inlet nozzle of the disturbed loop.

$$\Theta_{x,y,z}(t) = \frac{\sigma_{x,y,z}(t) - \sigma_0}{\sigma_1 - \sigma_0} \qquad \text{(Equ. 1)}$$

Θ represents the contribution of the coolant from the disturbed loop to the mixture at the given position x,y,z. The upper reference value σ_1 in (1) is the conductivity in the injected slug. The lower reference value σ_0 is the initial conductivity of the water in the test facility before the tracer is injected. The degree of mixing can be also expressed in relative boron concentration or temperature, if temperature measurement technique is applied.

The Vattenfall mixing test facility is a 1:5 scale model of a Westinghouse PWR [14]. The lower plenum and the lower 2/3 of the downcomer are made of acryl. A general view of the facility and the technological scheme of the model are shown on Fig. 3. Two idle loops are included in the model. The model is run with a maximum flow rate of 127 l/s and at temperatures between 20 and 50 ^{o}C. Components that can be important for mixing have been modelled, for example thermal shields, inlet pipe diffusers, structures in lower plenum, core support plates and core. The determination of the relative boron concentration is based on salt water tracering and conductivity measurement, too. Conductivity is measured to at 181 measurement positions close to the inlet to the core. A sampling frequency of 60 Hz has been used. The slug is injected into an empty section of the cold leg pipe that has been isolated from the rest of the pipe (between valves V4 and V5 in figure 3). The slug is released by quickly opening the two valves that encompass the slug (V4 and V5). Flow through the model is then slowly (during around 40 seconds) increased to the maximum flow rate. The increased flow rate is achieved by opening a motor gate-valve (V3) upstream of the slug. In order to

minimise buoyancy effects ethanol is added to the salt water to lower the density of the salt-water to that of tap-water. The density difference is lower than 1 kg/m^3 after this adjustment.

The test facility of EDO "Gidropress" [15] is a metal model of the Russian VVER-1000 reactor in a scale of 1:5. One loop with a loop seal and reactor coolant pump simulator is modelled. The other three loops are made short-circuit, and only the pressure loss of them is simulated. The core model has 151 fuel assembly (FA) simulators, which have the same pressure loss as the regular FA. Boron concentration change is modelled by a change in temperature (the de-borated water slug is simulated by colder water). About 100 thermocouples are placed in the lower part of the downcomer and at the core inlet to study the mixing of flows.

The Fortum PTS test facility [16] was a 1:2.56 scale model of the Loviisa VVER-440 reactor. The facility contained a half of the circumference of the reactor downcomer and included three cold legs and perforated plate in the lower plenum. The material of the facility was transparent acryl. The middle one of the three cold legs consisted of the section between RPV and RCP including the main gate valve and bottom safety injection point. Two other cold legs were built to model side loop flows only. The choice of the transparent material restricts the tests to atmospheric pressure and to a maximum temperature of around 75 °C. Minimum injection temperature was about 10 °C and the extra buoyancy effect was induced by salt addition to injection water. The high pressure injection (HPI) rate Q_{HPI}, side loop flows Q_A and Q_C, main loop flow Q_B as well as density difference ratio between HPI and loop flow water were varied. Most of the 62 thermocouples were installed to the downcomer to measure the temperature fluctuations on the vessel wall. The thermocouples were read once in two seconds. A schematic view of the facility is shown in Fig. 4 .

C.2.2. Slug mixing tests

The slug mixing test matrix contains 12 experiments at ROCOM and 4 experiments at the Vattenfall facility with simulation of the start-up of the first main coolant pump. The test matrix is shown in Table I. A detailed description of the experiments and their results is given in [1]. The measurement data are documented in [27] and [28].

For the pump start-up experiments the following boundary conditions were varied:

- Length of the pump ramp
- Final mass flow rate of the loop with the starting–up pump
- Volume of the unborated slug and initial position in the cold leg
- Status of the unaffected loops
- Geometry of the reactor pressure vessel

The experiments ROCOM-02 and VATT-04 represent the basic scenarios of pump start-up for the both facilities. In that cases, the transit time for the slug, i.e. the time it takes for the slug to travel from its initial position to the inlet to the core, is the same as in the plant. The other three Vattenfall tests cases are run with a higher flow rate in order to increase the Reynolds number, and thereby decrease the Reynolds number scaling effects. Strouhal number scaling is used to determine the ramp length for these tests.

A series of experiments are made for different slug sizes (ROCOM-01; -02, -03 and –12; VATT-01; VATT-02 and –03). The impact of the initial slug position was investigated in experiments ROCOM-04, -05 and –06 versus ROCOM-03. Strouhal scaling was considered in tests ROCOM-08 and –09 versus ROCOM-03. The final flow rate after the pump start-up was varied in ROCOM-10 and –11. ROCOM-07 was performed to estimate the influence of the status of the idle loops. Besides of the measurements of boron concentration at the inlet to the core, laser Doppler velocimetry (LDV) measurements of vertical and tangential/circumferential velocity in the downcomer during steady state and transient conditions were performed at both test facilities.

Fig. 5 shows the time evolution of the mixing scalar at the two sensors in the downcomer in the ROCOM-02 slug mixing test. Both sensors are shown in an unwrapped view. From this visualization is clearly to be seen, that the de-borated coolant passes around the core barrel instead of flowing directly downstream. At the upper sensor, the tracer arrives still below the affected inlet nozzle. With growing time, the tracer spreads in the azimuthal direction. Subsequently, at the lower sensor two maximums of the tracer at azimuthal positions on the back side of the downcomer are observed. Therefore, the tracer arrives at the core inlet plane first at positions, which are opposite to the position of the loop with tracer injection. A similar mixing pattern being typical for slug mixing during start-up of the first pump was also observed in the Vattenfall experiments.

The mixing scalar distribution at the core inlet at the moment of maximum tracer concentration resp. minimum boron concentration for the experiments ROCOM-02 and VATT-02 are shown on Fig. 6. Please note, that in the two figures the quantification of mixing degree is given in different presentations. For ROCOM-02, the mixing scalar is shown, while for the VATT-02 test the normalized minimum boron concentration is depicted. The minimum boron concentration is unity minus the mixing scalar. Fig. 6 shows, that the maximum dilution is reached in the half of the core opposite to the sector where the loop with slug injection is located. However, the distribution is more asymmetric in the Vattenfall experiments. It is assumed, that this asymmetry is caused by an asymmetric velocity profile at the inlet nozzle, as it has been proved from CFD calculations. In the Vattenfall facility, a bend is existing in the cold leg pipe not far upstream from the inlet nozzle. This bend causes a distortion of the flow velocity distribution in the inlet nozzle plane leading to a velocity field deformation in the downcomer. Velocity measurements under steady-state flow conditions with one working pump in the lower part of the downcomer have shown, that the azimuthal velocity distribution along the perimeter of the downcomer is very asymmetric. At some positions, the vertical velocity component is even positive, that means there is an upwards flow. Moreover, velocity value at this position was found to be very strongly fluctuating in time. The complicated and fluctuating velocity field leads to the asymmetric, complicated mixing pattern at the core inlet.

As it was mentioned above, the length of the pump ramp, final mass flow rate of the loop with the starting pump, volume of the injected slug and initial position in the cold leg as well as the status of the unaffected loops was varied in the experiments. Some aspects of the influence of these variations on the mixing will be discussed in the following only briefly in a qualitative manner. In the experiments ROCOM-01; 02; 03 and 12, as well as in VATT-01, VATT-02 and VATT-03, the initial slug size was varied. All other boundary conditions are identical. It was proved, that with growing slug volume, the maximum value of tracer concentration reached in the experiment is growing, too. This has been proved for both facilities. Only

between ROCOM-02 (20 m^3) and ROCOM-01 (40 m^3) the maximum value is no more increasing, because due to the decreasing tracer concentration during the injection, the rear part of the slug does no more contribute to the maximum mixing scalar, in spite of the fact, that the overall salt volume input is greater (volumes related to original reactor geometry).

In the experiments ROCOM-04; -05 and -06, the influence of the initial slug position was investigated. The initial distance of the slug from the pressure vessel was varied from 2.5 m until 40 m (related to the original reactor geometry) in these experiments (see table I). Fig. 7 compares the distributions at the time point of maximum mixing scalar at the core inlet for all four experiments with variation of the initial slug position. As it can be concluded from that figure, with increasing initial distance, the location of the maximum at the core inlet moves to the side opposite to the starting loop position. Further, the first experiment shows a significantly lower maximum value. That indicates, that a qualitative change of the flow conditions takes place during the pump start-up process. The typical velocity field, being responsible for the maximum at the opposite side of the core inlet cross section, establishes with a time delay of some seconds, only. Therefore, slugs entering the vessel at an early stage of the process, flow more or less directly downwards, instead of flowing to the opposite side. In the initial stage of the mass flow increase, there is a slug-like movement of the whole liquid inside the RPV, while later two large vortexes are formed in the two parts of the downcomer left and right from the starting loop position.

Complementary experiments on slug mixing were performed at the VVER-1000 mixing test facility [30]. A slug of low borated coolant was assumed to be accumulated in the cold leg loop seal located before the main coolant pump. The boron concentration in the reactor model was studied using the temperature method. The borated primary coolant was simulated by hot water at temperature of 65-75 ^oC, the un-borated slug – by cold water at temperature of 20-30 ^oC. The water volume in model loop seal was equivalent to 8.5 m^3 in the full-scale reactor. The circuit was heated up due to the heat released during operation of the circulation pump. After heating up, the pump was shut down and the gate valves at the loop seal inlet and outlet were closed. The hot water between the valves was replaced by colder one. The experiment was then started opening the valve in the moment of pump start-up. The mixing pattern at the core inlet was obtained from temperature measurements. Three series of tests with final flow rates of 175; 470 and 815 m^3/h and pump start-up times of 2, 8 and 16 s and without back flow through the idle loops were carried out. Each series of the experiments consisted of five or six experiments for statistical averaging. The results confirm qualitatively the findings from the ROCOM and Vattenfall tests, but cannot directly be compared due to differences in the geometry of the facilities and in the boundary conditions of the experiments (compare fig. 8 and 25, section C.4.5).

C.2.3 Experiments on buoyancy driven mixing

For the investigation of the influence of density effects, generic experiments have been carried out at the ROCOM test facility. It is expected, that density differences can be neglected, if the flow rates are sufficiently high, that means, if mixing is momentum controlled. The objective of these experiments was to find the conditions for transition from momentum controlled mixing, as it is typical for pump start-up scenarios, to buoyancy driven mixing, being relevant for PTS scenarios and natural circulation re-start after LOCA. Specific PTS mixing experiments has were performed at the Fortum PTS test facility.

Due to the fact, that the ROCOM facility cannot be heated up, the necessary density differences were simulated by adding sugar (glucose) to the water that is injected into the cold leg. To observe the mixing of the ECC water fed into the cold leg by the HPI system, this water was tracered by small amounts of sodium chloride, as in previous experiments. Generating density differences by high salt concentrations is not possible, because the measurement system is very sensitive and would be saturated at high salt concentrations. An accurately modelled ECC injection nozzle has been connected to one of the cold legs of ROCOM from side under an angle of 60°. At the Fortum PTS facility, the colder water was injected from the bottom of the cold leg of the test facility. The mixing of the injection water was then observed by measuring temperatures in the downcomer and in the cold leg and visually through the transparent material of the facility. The density difference of the colder HPI water was further induced by salt addition. The density difference ratios between HPI and loop flow used in the tests was $(\rho_{HPI} - \rho_L)/\rho_{HPI} = \Delta\rho/\rho = 0.022 - 0.16$. In the ROCOM tests, a maximum density difference of 10 % was generated. Table II gives a comparison of the features and parameters of the two facilities.

The goal of the ROCOM experiments was the generic investigation of the influence of density differences between the primary loop inventory and the ECC water on the mixing in the downcomer. To separate the density effects from the influence of other parameters, a constant flow in the loop with the ECC injection nozzle was assumed in this study. The mass flow rate was varied in the different experiments between 0 and 15 % of the nominal flow rate, i.e. it was kept in the magnitude of natural circulation. The other pumps were switched off. The density difference between ECC and loop water has been varied between 0 and 10 %. In the Fortum PTS facility, experiments have been performed with coolant mass flow in the loops adjacent to the HPI loop. At ROCOM, only the HPI loop was operated. Table III summarises the boundary conditions of the ROCOM experiments and selected Fortum PTS tests. In table III, only Fortum PTS tests with zero flow rate in the adjacent loops are included.

Altogether 20 experiments have been carried out at ROCOM. In all experiments, the volume flow rate of the ECC injection system was kept constant at 1.0 l/s. The normalised density is defined as the ratio between the density of water in the ECC loop and density of fluid in the circuit. All other boundary conditions are identical. Due to the observed fluctuations of the flow field in the RPV, each experiment was repeated five times to average over these fluctuations. In the following, the experiments are classified by the nomenclature DxMy, where x is the percentage of density difference and y is the percentage of nominal mass flow rate in the cold leg.

The experiments without density effects serve as reference experiments for the comparison. Fig. 9 visualises in unwrapped views the time evolution of the tracer concentration measured at the two downcomer sensors. The downwards directed bold arrow indicates the position of the loop with the running pump, in that case delivering 10 % of the nominal flow rate. In the left figure, the results from experiment D00M10 (#12 according to table III) are shown. No density difference was created. At the upper downcomer sensor, the ECC water (injected in each experiment from t = 5 to t = 15 s) appears directly below the inlet nozzle. Due to the momentum created by the pump, the flow entering the downcomer is divided into two streams flowing right and left in a downwards directed helix around the core barrel. At the opposite side of the downcomer, the two streaks of the flow fuse together and move down through the measuring plane of the lower downcomer sensor into the lower plenum. Such a flow

distribution is typical for single-loop operation. It is dominated by the momentum insertion due to the operating pump or high natural circulation flow rate. The maximum tracer concentration of the ECC water in the downcomer is 20 % of the injected water concentration at the upper sensor and 8 % at the lower sensor. Fig. 9 (right) shows the experiment #17 (D10M10), carried out at the same flow conditions, but the density difference between the injected ECC water and the primary loop coolant is now 10 %. In that case a streak formation of the water with higher density is observed. At the upper sensor, the ECC water covers a much smaller azimuthal sector. The density difference partly suppresses the propagation of the ECC water in horizontal direction. The ECC water falls down in an almost straight streamline and reaches the lower downcomer sensor directly below the affected inlet nozzle. Only later, coolant containing ECC water appears at the opposite side of the downcomer. The visualisations of the behaviour of the ECC water in the downcomer reveals that in case of momentum driven flow, the ECC water covers nearly the whole perimeter of the upper sensor and passes the measuring plane of the lower sensor mainly at the opposite side of the downcomer. When the density effects are dominating, the sector at the upper measuring device covered by the ECC water is very small. The ECC water falls straight down and passes the sensor in the lower part of the downcomer below the inlet nozzle of the working loop. Furthermore, variations of the density were carried out to identify the transition region between momentum driven and density driven flow.

Based on these observations, the set of experiments conducted according to table III, was divided into three groups: density dominated flow (◊), momentum dominated flow (Δ) and the transition region (*). The conditions at the inlet into the downcomer were used to calculate Froude-numbers of the experiments according to the following formula:

$$Fr_{DC} = \frac{v_{in}}{\sqrt{g \cdot H \cdot \frac{\rho_{in} - \rho_a}{\rho_{in}}}} \qquad \text{(Equ. 2)}$$

where v_{in} is the velocity at the reactor inlet (combined loop and ECC flow), g is the gravitational acceleration, H is the height of the downcomer, ρ_{in} the density of the incoming flow, calculated with the assumption of homogeneous mixing between ECC and loop flow, and ρ_a the density of the ambient water in the downcomer. Lines of constant Froude-numbers calculated by means of this formula are shown in Fig. 10. All experiments, identified as density dominated are located in the region left of the isoline *Fr = 0.85* and all momentum dominated points are found right of the isoline *Fr = 1.5*. Therefore, *Fr = 1* is about the critical Froude number separating the two flow regimes for the ROCOM test facility. Around this critical Froude number a transition region is located.

Density effects are extremely developed in an experiment with no flow in the primary loop (Fig. 11), where the fluid circulation is initiated only by starting the ECC injection. At the upper sensor, the ECC water appears unmixed and covers a sector of only about 15 degrees. The data from the lower downcomer sensor show clearly buoyancy induced turbulent structures. As can be concluded from these data, the water with higher density accumulates in the lower plenum.

Applying the same Froude scaling as it is given in equ. (2), all Fortum PTS tests are located in the density driven mixing region.

In the Fortum experiments, additionally the mixing in the cold leg due to the HPI injection was investigated. When the flow in the main loop is maintained by the natural circulation, nearly ideal mixing of HPI injection water is obtained. However if the loop flow is stagnant the mixing is not complete, and stratification and buoyancy driven re-circulation dominate the behaviour of the system [16]. The mixing of the HPI water in the injection point depends on the injection Froude number and the injector geometry. A quantitative criterion of this mixing is the so-called backflow ratio. The backflow ratio $Q^* = Q_h/Q_{HPI}$ is defined as the ratio between the flow rates of the stratified colder layer in the bottom of the cold leg flowing to the downcomer and the counter-flowing hot stream from the downcomer ("backflow Q_h"). Q* has been calculated from the temperature data of the experiments. Fig. 12 presents the dependence of the backflow ratio from the modified Froude number [16]:

$$Fr_{CL,HPI} = \frac{Q_{HPI} / A_{CL}}{\left(gD_{CL}\Delta\rho_{HPI} / \rho\right)^{1/2}} . \qquad \text{(Equ. 3)}$$

Q_{HPI} is the injection flow rate, A_{CL} the cross section of the cold leg, D_{CL} – the diameter of the cold leg, $\Delta\rho_{HPI}$ the density difference between HPI water and cold leg flow. The Froude number definition of equation (3) contains characteristic parameters for the HPI injection mixing, while the Froude number according to equ. (2) is related to the downcomer parameters. A high back flow ratio means strong stratification, low back flow ratio indicates better mixing. The back flow ratio is a parameter to be compared with results from the CFD validation calculations.

On fig. 13, the time evaluation of the concentration of the HPI water averaged over all measurement points at axial position 164 mm below the inlet nozzles in test 10 is shown. The comparison with analytical full mixing curve shows, that mixing in that region is weak.

C.3 Steady-state mixing and flow distribution (WP 3)

C.3.1 ROCOM steady-state experiments

Flow distribution in the primary circuit of the PWR is an important issue connected to many operational problems. The temperature profile at the core outlet, relevant for the determination of the reactor power and thus for economical plant operation, is directly influenced by the flow distribution at the core inlet. Also the quasi-steady flow with macroscopic oscillating swirls inside the reactor vessel can cause temperature fluctuations and therefore is of importance to long-term thermal fatigue. Besides of normal operating conditions, the study of mixing under steady state conditions is important for overcooling transients, when all pumps are running, but the cold leg temperature is much lower in one of the loops

Steady state mixing and flow distribution measurements have been performed at the ROCOM test facility. The matrix of experiments is shown in table IV. It comprises 9 experiments with various combinations of running pumps, while the idle loops are open for back flow, and various mass flow rates in the working loops. As it was mentioned in the introduction, the study of mixing under steady state conditions is important for overcooling transients, when all pumps are running, but the cold leg temperature is much lower in one of the loops (experiment ROCOM-stat01). To check the mixing pattern in the case of fully developed

natural circulation, the mass flow rate in all loops were reduced in one experiment (ROCOM-stat02). The flow distribution in the case of different combinations of running pumps is of interest for operational states during reactor start-up procedure (ROCOM-stat03, -stat04, -stat05, stat06, -stat07). Two cases with an asymmetry of 10 % and 20 % in the flow rates between two loops are considered being of interest from the viewpoint of NPP operation, where loop flow rate differences can occur (ROCOM-stat08, -stat09). The measurement data are documented in [29].

Because mixing experiments cannot be performed under real steady-state conditions with permanent tracer injection, the following approach was applied. A sufficiently large slug of tracer solution was injected assuring "saturation" in the sense, that the tracer distribution is nearly constant at the core inlet for some time. If the injection time is too short and the tracer slug is too small, the mixing along the stream lines leads to reduction of the maximum tracer concentration in comparison with the "saturation" value. On the other hand, if the slug is too large, it will turn around the whole circuit, and the front of the slug comes back to the core inlet a second time still during continuation of the injection. In the experiments, considerable fluctuations of the tracer concentration distribution at the core inlet have been observed. They are due to macroscopic turbulent fluctuations of the velocity field. Therefore, the measurement data from 5 repeated realizations of the same experiment were used for averaging. The averaging was performed individually for all four sensors over the time interval, when the mixing scalar was nearly constant at plateau level.

The averaged mixing scalar distribution in the measurement planes is shown on fig. 14 (left). The mixing scalar is almost homogeneously distributed in the cold leg pipe cross section at the RPV inlet. In the downcomer and in the core inlet plane a sector formation is seen. An isoline plot of the mixing scalar is shown in fig. 14 (right). The maximum mixing scalar value is 0.94. That means, a part of the tracer reaches the core inlet plane almost un-mixed. The sector becomes more and more smeared on the way from the inlet nozzle to the core inlet. This is caused not only by turbulent dispersion in the flow, but also by turbulent fluctuations of the velocity field.

Besides of tracer concentration measurements according to the measurement technology described in section C.2.1, measurements of the velocity field in the downcomer were performed by applying laser Doppler anemometry in most of the experiments. The measurement data was also made available for the validation of CFD methods. The steady state experiment with only one loop in operation represents the final state for the slug mixing test with start-up of the first pump. The measured velocity distribution around the perimeter in the lower part of the downcomer is shown on fig. 15 (left). An illustrative picture of the velocity field is shown in the right part of the figure. It can be seen, that there are minima of the vertical velocity component at positions below the inlet nozzles, while the maximums are located between the inlet nozzle positions. The jets from neighbouring loops impinging on the core barrel and move downwards meet at that positions. The velocity fluctuations measured by the LDV device were used to get the uncertainty band of the velocity measurement shown on the left figure.

Concerning the effects investigated in the 9 different experiments of the test matrix, only the case of asymmetric loop flow, when all pumps are running, will discussed in the following. This effect was investigated in experiments ROCOM-stat08 and ROCOM-stat09 with 10 % and 20 % asymmetry between two neighbouring loops. Fig. 16 shows in the left part the time

evolution of the mixing scalar in the downcomer, in the right part the mixing scalar distribution at the core inlet in experiment ROCOM-stat09. In this case of only 20 % mass flow rate asymmetry, the mixing pattern has significantly changed. The sector with high mixing scalar values is extended to more than 90 degrees, because the mass flow rate in the loop with tracer injection is higher than in the other ones. Further, at the core inlet a second maximum appears in the distribution. The splitting of the tracer already starts in the lower part of the downcomer. Due to the asymmetry in the flow rates, the distribution of the tracer is comparable with an experiment with tracer injection into two loops. The velocity field in the downcomer is responsible for this splitting. The results show, that the velocity field and the mixing pattern are very sensitive to the inlet flow boundary conditions.

C.3.2 Measurements at NPP

Experimental investigations on flow distribution and coolant mixing under steady-state conditions have also been performed at nuclear power plants. In the 70ties, first measurements were carried out at the Loviisa and Sizewell power plants (e.g. [17]. Experiments at the Paks VVER-440 NPP were carried out in 1987-1989 during commissioning tests of newly replaced safety valves of the steam generators [18]. A series of 60-80 experiments was performed at about 10-15% of reactor power, where the main steam line valve of one steam generator was closed causing the heat-up of the corresponding loop. After some time, by slow increase of the reactor power, the safety valve of the steam generator was forced to open. At the moment just prior to the opening of the safety valve the cold leg temperature of the investigated steam generator were by 8-9^{o}C higher than that of the others, while the heat-up of coolant in the reactor in this cases was only 3-4^{o}C. Therefore, a significant asymmetry in the core outlet temperature distribution was caused and measured by the 210 thermocouples, located in the fuel assembly heads. Analysing the date from 12 experiments under different conditions, where some of them have been repeated several times, mixing matrices have been derived by linear regression analysis.

These matrices describe the fraction of the perturbation of the coolant temperature in one primary circuit loop assigned to each fuel element (6 matrices - one for each loop of the VVER-440). The maximum mixing coefficients in any case are not below 75%. The absolute error of the matrix coefficients was evaluated to about 3%. A symmetry perturbation of the mixing matrices was found caused by internal structures in the downcomer (coolant baffles aimed at directing the emergency core cooling water from the hydro-accumulators to the core). No swirling, as it as was observed in earlier experiments at the NPP Loviisa, was found in the Paks measurement results (see Fig. 17). This is probably due to the different constructions of the main coolant umps in both NPPs. The measurements at NPP Paks confirm qualitatively the results obtained at ROCOM, although the geometry of the RPV and its internals is quite different in the corresponding reactor types. Mixing under steady state conditions is quite incomplete. The degree of mixing is quite higher in the slug mixing case due to the high momentum insertion caused by the pump start-up.

The mixing data from the real reactor are very important, because the comparison of this data with CFD results provides information about real uncertainties in the CFD reactor calculations, which are not only due to model errors and numerical errors of the CFD code, but also due to uncertain information e.g. on boundary conditions, uncertainties of the measurement technology, uncertainties in real geometry and other uncertainties, which can be minimized in the tests at the experimental facilities, but not in the real reactor. Another

advantage is the real scale of the tests. However, the measurement error is certainly higher in the real reactor.

C.4. CFD code validation

C.4.1 Application of the Best Practice Guidelines for CFD

The main objective of FLOMIX-R WP4 (Work Package 4) is to investigate how well mixing during boron dilution transients in PWRs can be modelled by Computational Fluid Dynamics codes. The competitiveness of CFD is continuously growing due the rapid developments in computer technology. Computer capacity is still, and will be for a foreseeable future, a limiting factor for the capacity for CFD calculations to produce completely accurate results. Simplified models for describing turbulence therefore have to be used and the computer capacity put restrictions on the resolution in space and time that one can use in a CFD calculation. This leads to modelling errors and numerical errors that give more or less inaccurate results. Validation of the quality and trust of different approaches in CFD calculations are therefore needed. In FLOMIX-R WP4 validations of CFD calculations have been made against experiments for boron dilution transients performed in four different test facilities and measurement data from NPP.

Calculations in WP4 have been made by the following partners: FZR, GRS, FORTUM, PSI, Vattenfall Utveckling, NRI, VUJE, AEKI, Budapest University and NRG. The commercial CFD codes CFX4, CFX5 and FLUENT6 have been used [19], [20], [21] and [22]. CFD calculations have been made for the following tests:

- ROCOM (Rossendorf Coolant Mixing Model) test facility (1:5 scale German Konvoi PWR).
  - Steady state mixing cases ROCOM-stat01, -stat04, -stat08 and -stat09.
  - Transient slug mixing cases ROCOM-01, ROCOM-02, ROCOM-03 and ROCOM-08
  - Transient buoyant slug mixing case D10M05 and D05M00

- Vattenfall test facility (1:5 scale Westinghouse PWR)
  - Steady state non-mixing case VATT-02
  - Transient slug mixing case VATT-02

- FORTUM PTS test facility (2/5-scale VVER-440 PWR)
  - Buoyant steady state mixing case 20
  - Buoyant transient cases 10, 20 and 21.

- GIDROPRESS test facility (VVER 1000 PWR)
  - Buoyant transient slug mixing test 1 and 2.

- PAKS NPP tests (VVER-440 PWR)
  - Data from the commissioning tests.

The CFD code validation was focussed mainly on a number of benchmark cases from the steady-state mixing experiments, slug mixing tests and experiments with density differences.

So-called Best Practice Guidelines (BPG) were used for quality assurance of the validation calculations. ERCOFTAC BPG [23], [24], which have been specified for nuclear reactor safety calculations within the ECORA project [25] were applied. The BPG are built on the concept of an error hierarchy. The different types of errors in CFD simulations are divided into the two main categories:

- Numerical errors, caused by the discretisation of the flow geometry and the model equations, and by their numerical solution
- Model errors, which arise from the approximation of physical processes by empirical mathematical models

This concept implies that numerical errors are quantified and reduced to an acceptable level, before comparison with experimental data is made. The BPG contain a set of systematic procedures for quantifying and reducing numerical errors. The knowledge of these numerical errors is a prerequisite for the proper judgement of model errors. The separation of numerical errors from model errors allows then valid conclusions on model performance. Numerical errors are minimised by optimising the computational mesh, numerical schemes, convergence criteria and time step. Another kind of errors are uncertainties rising from insufficient information about the problem definition and set-up. These uncertainties can be quantified by performing calculations with variations on the unknown parameters and by a sub-sequent analysis on the influence of these parameters. This belongs to boundary positions, boundary conditions and internal geometry modelling. Turbulence models are the most relevant physical models responsible for model errors. Only if sensitivity tests are made the solution errors and model errors can be quantified and only then you can get an indication on how good your CFD calculations are. Sensitivity tests for the following aspects were considered:

- Grid size
- Convergence criteria
- Round-off error
- Time-step size
- Turbulence model
- Inlet boundary position and inlet boundary condition
- Outlet boundary position
- Internal geometry
- Code

Fig. 18 shows examples for computational grid and time step optimisation using the CFX-5 code. The number of mesh points for the discretisation of the solution area has to be increased until convergence of the solution has been achieved (mesh with about 750.000 elements using the Upwind Discretisation Scheme UDS). The same procedure has to be applied concerning time step refinement (see also fig. 18).

However, in practical applications with complicated geometry and complex flow phenomena like the mixing problems considered, a really grid and time step independent solution can often not be reached by practical reasons (computer resources). In these cases, so called production meshes were used in the calculations. The production mesh is an optimum between maximum possible refined grid on the one hand, but with omitting parts of the flow domain, which were found to be of small impact on the results, e.g. the cold leg loops. The

production mesh is not yet a mesh, for which grid-independent solution was reached. In general, the choice of the production mesh is dependent from the process to be simulated. The production mesh for momentum driven mixing calculations might be different from that one for the analysis of buoyancy controlled mixing. The production mesh for the CFX-5 calculations was an unstructured grid with about 7 million elements (see fig. 20).

Concerning numerical solution schemes, higher order schemes are preferred due to higher accuracy. Fig. 19 shows the velocity distribution (vertical component) in the core inlet plane calculated with the FLUENT code for steady state conditions with one running pump in the Vattenfall facility by applying first order and second order scheme. Using the first order scheme, the solution is well converging, but physically wrong. The position of the maximum velocity observed in the experiment is not met in the first order solution. The reason is to be seen in the influence of inlet boundary conditions. The bend in the cold leg pipe not far from the RPV inlet nozzle causes an asymmetric velocity profile and turbulence parameters distribution at the RPV inlet. This impact of the bend is not well reproduced in the more diffusive first order scheme calculation. The disturbance caused by the bend is not "transported" to the core inlet plane, the diffusive scheme "forgets" about it.

C.4.2 Post-test calculations of ROCOM steady state mixing tests

CFX calculations have been performed by GRS and FZR. The CFD codes used at FZR are CFX-4 and CFX-5. A baseline steady-state calculation of ROCOM-stat01 using CFX-5.6 was performed by GRS. The main aim of this calculation was to investigate systematically numerical and model errors by analysing the mesh influence, different discretisation schemes, the location of the flow boundaries, the flow resistance in the lower plenum and different turbulence models. Results of investigations on the convergence of the velocity filed in the downcomer are presented in section C.4.1. Details of the results are given in Appendix 2 of Deliverable D11 [3].

Fig. 21 shows a comparison between CFD solutions and experiment for a ROCOM steady state mixing test with four running pumps. The sector formation and the high maximum mixing scalar values are well reproduced in the calculation. The best agreement was achieved, when a transient calculation for the steady-state conditions was performed, because the velocity field in the flow domain is not really time-independent even with steady-state boundary conditions. Macroscopic fluctuations occur, which are averaged from the transient solution.

Parallel to CFX, the CFD code FLUENT has been used for performing second code calculations for the basic steady state mixing test ROCOM-stat01 and for calculating additional steady state tests with asymmetric operation of loops. The tests ROCOM-sta01 and ROCOM-stat04 have been calculated by VUJE. AEKI calculated ROCOM-stat01 and –stat09. Second code calculations are an important contribution with respect to different mesh structures, specific turbulence models and particularly for modelling of internal structures. A comparison of the different FLUENT and CFX-5 results with measurement data (plateau averaged mixing scalar distribution at core inlet) for ROCOM-stat01 is also shown on fig. 21. The results of the calculations for the additional tests ROCOM-stat04 and ROCOM-stat09 are described in D11 [3].

The velocity field in the downcomer shows a qualitatively good agreement between the CFX-4 and CFX-5 calculations and the experimental results (LDA measurements at ROCOM [11]).

Particularly, the calculations confirm the location of minimum flow velocities below the inlet nozzles found in earlier experiments [26]. A maximum velocity exists at azimuthal positions between the two inlet resp. the two outlet nozzles. A comparison between measured and calculated velocity distribution in the lower downcomer is shown in fig. 22. The calculated and measured velocity distributions agree mostly within the uncertainty band of the measurements, with exception of the velocity minimum at 45 degrees (loop 1). There is obviously a deviation from the symmetry to be expected in the measured velocity field due to equal mass flow rates in all loops. A measurement error of this magnitude in the mass flow rates can be excluded. However, in loop 1 the mixing device for the tracer injection was installed. The mixer creates an additional flow resistance, which was taken into account by adjustment of the pump head in this loop. It is assumed, that the mixer affects the velocity profile, distribution of turbulence or occurrence of swirls induced by the pumps in the corresponding cold leg pipe, what may have an impact on the velocity distribution. However, this assumption could not be checked because velocity measurements near the RPV inlet were not possible.

In general, the flow pattern, velocity distribution in the downcomer and mixing scalar distributions at the core inlet are qualitatively well predicted in the CFD calculations. The velocity field in the downcomer has inhomogeneous character with maximum downwards flow components in the regions in-between the inlet nozzles. A clear sector formation of the flow in the downcomer is seen. This leads to maximum mixing scalar values at the core inlet of 92 – 99 %. That means, a part of the fluid remains almost unmixed. The re-distribution of the velocity field and mixing scalar distribution in the case of asymmetric flow conditions is also qualitatively well reproduced in the calculations.

Finer grids in the CFD simulation tend to give better results. Also modelling of perforated sheets (such as the drum in the downcomer) as real structure rather than porous medium improves quality of results. Influence of porous medium as a substitute of a perforated sheet can be, in some extent, controlled by proper definition of direction-dependent resistance of the porous medium. Other investigated effects (turbulence model, wall function, position of outlet boundary) do not have an unambiguous influence on results. In general, the mixing along the flow path in the downcomer is under-predicted in all calculations. Disturbance in the inlet boundary conditions has significant impact on the flow pattern. This can be seen in experiment ROCOM-stat01, where a disturbance in turbulence or swirl intensity caused by the mixer is assumed to be responsible for an observed perturbation in the velocity distribution.

C.4.3 CFD calculations for the ROCOM slug mixing tests

The CFD calculations for ROCOM slug mixing tests were carried out with the CFD codes CFX-4, CFX-5 and FLUENT. The transient slug mixing cases ROCOM-01, ROCOM-02, ROCOM-03 and ROCOM-08 were calculated. Focus was put onto the benchmark case ROCOM-02. A second code calculation was performed for this case with FLUENT. In this report, only the calculations for the ROCOM-02 case will be summarized. A detailed description of all the calculations and their results is given in D11 [3].

CFX calculations

The specific situation concerning CFX was, that during the duration of the project the code was undergoing an enormous development. The code versions CFX-4 and CFX-5 are practically completely different codes, concerning the code philosophy, the physical models, the numerics, pre- and post-processors. CFX-4 uses a block-structured mesh. The meshing philosophy for CFX-5 was initially based on un-structured, tetrahedral meshes. With the development of a new, CAD based pre-processor ICEM-CFD, hybrid meshes can be used with all kinds of unstructured elements, like prisms, tetrahedrals, hexahedrals, wedges etc.. Due to the specific situation with CFX, a broad variety of calculations was performed using CFX-4 and CFX-5. 11 different grid types were generated and used in the CFX-5 calculations. In the CFX-5 calculations, all internals were modelled in detail. No porous body approach was applied. All the 194 orifices in the core support plate were modelled. The perforated drum in the lower plenum contains 410 orifices of 15 mm diameter. A model with a reduced number of holes (90 holes) and a complex model using all 410 holes was used as a result of extensive sensitivity tests analysing the influence of the perforated drum of the flow field and mixing in the lower plenum.

Based on the meshing studies, finally two grid types (production meshes) were used for the basic calculations: the tetrahedral production mesh (Grid 5, about 7 millions elements) and the hybrid production mesh (Grid 9 with 4 million elements). The production mesh is an optimum between maximum possible refined grid on the one hand, but with omitting parts of the flow domain, which were found to be of small impact on the results, e.g. the cold leg loops. The production mesh is not yet a mesh, for which grid-independent solution was reached. This could not be fully achieved. In general, the choice of the production mesh is dependent from the process to be simulated. The production mesh for momentum driven mixing calculations might be different from that one for the analysis of buoyancy controlled mixing. Modifications of these grid types were used for further investigations (outlet boundary position, modelling of one cold leg or all four cold legs, inlet boundary position at the cold leg nozzle etc.).

In the CFX-5 production mesh, all holes in the sieve drum are modelled. Inlet boundary position is at the inlet nozzle, outlet boundary at half height of the core. Both production meshes are suitable for the post test calculation of basically all ROCOM experiments, with slightly preferences of the tetrahedral production mesh for the steady state mixing experiments and the hybrid production mesh for the slug mixing and density driven experiments. Because no full grid independence was achieved, there are differences in the results obtained with different mesh types.

Figure 23 shows streamlines representing the velocity field in the downcomer and lower plenum (including the perforated drum and lower support plates as porous media) at the pump start-up scenario calculated with CFX-4. Due to a strongly momentum driven flow at the inlet nozzle the horizontal part of the flow dominates in the downcomer. The injection is distributed into two main jets, the so-called butterfly distribution. In addition, several secondary flows are seen in various parts of the downcomer. Especially strong vortices occur in the areas below the non-operating loop nozzles and also below the injection loop.

Fig. 24 shows a quantitative comparison between CFD solutions and experiment for the slug mixing test ROCOM-02. The time behaviour of the maximum mixing scalar value at the core inlet is shown. The CFX-4 and CFX-5 solutions are compared with the measurement. The statistical error of the measurement data (error band P2 of two standard deviations) is shown obtained from the averaging of the data from five repetitions of the same experiment. This

statistical error is not the measurement error, but is caused by macroscopic fluctuations in the flow. The CFD solutions are not always within the uncertainty band of the measurements, but the relevant values of maximum mixing scalar (safety relevant minimum boron concentration) are close together.

FLUENT calculations

A transient calculation of the ROCOM slug mixing experiment ROCOM-02 was performed by FORTUM using the code FLUENT-6. Similar settings were, if possible, used in both codes. Due to limits in computational resources the mesh of the 2nd code calculation was coarse, internals were simplified and the core region was not modelled at all. The mesh had therefore accuracy limitations. The perforated drum was modelled as porous media with resistance coefficients. The core support plate was modelled in detail, the outlet boundary was placed on the top of core support plate. The unstructured mesh contains 363106 nodes and 1846679 elements. A grid independent solution of the pump start-up slug mixing experiment with the "2nd code calculation mesh" was not achieved. Differences in the mixing behaviour of the slug occur, which are in a range of max. 13% of the averaged values at the time of the maximum compared to the loop value, differences at selected local positions appear to be larger than the averaged values. Nevertheless, the global qualitative mixing pattern of the experiment in the downcomer and core inlet could be observed in the two CFD codes. Although similar setting were used, the solutions still strongly depend on the used solver algorithms.

Conclusions

The qualitative and quantitative agreement of the CFD calculations with the corresponding experiments is very good for steady state flow case ROCOM-stat01 and acceptable for the pump-start-up case ROCOM-02.

Sensitivity studies have shown, that the SST turbulence model and the automatic wall functions together with higher order discretization schemes should be used if possible.

From the second code analysis the conclusion was drawn, that prior to inter-code comparison of the results, a grid-independent solution should be obtained with each code according to the Best Practice Guidelines.

C.4.4 Quantitative Comparison of CFD results with measurement data for the ROCOM non-buoyant experiments

For the assessment of agreement between calculation and measurement, not only visual and qualitative comparisons have to be performed, but also a quantitative estimation of the deviations. Deviations between calculation and measurement occur due to model errors, e.g. in turbulence modelling, but also due to uncertainties in conditions of the experiment, e.g. uncertainties in geometry, boundary conditions or measurement error. Comparison between calculation and experiment should be performed after minimizing numerical errors according to Best Practice Guidelines [25]. So called "best practice solutions" were included into the comparison, where numerical errors are reduced to maximum possible extend. Target values and comparison criteria have been evaluated by B. Hemström (Appendix 11of D11 [3]). This methodology is applied in the following for quantitative assessment of deviations between calculation and experiment.

For the quantitative comparison of the experimental and calculation results, three stationary experiments and one transient experiment at the ROCOM test facility were selected. The comparison was made between the calculated and measured data of the mixing scalar in the core inlet plane of the test facility. In this plane, 193 measurement positions are installed, one at the entry into each fuel assembly. Exactly at these positions, the calculated values for the mixing scalar were extracted from the calculations.

For the quantitative comparison different types of deviations were defined. These are

$$DEV1_{i,t} = c_{c,i,t} - c_{m,i,t} \qquad \text{(Equ. 4)}$$

where c_c is the calculated and c_m the measured value of the mixing scalar or the velocity at the position i and the time t. DEV2 is an accumulated deviation at the certain position i over the important time span, i.e. when the perturbation is moving through the measurement plane. Two representations of the accumulated deviation were selected, the first is the absolute deviation.

$$DEV2_i\_ABS = \sum_{t=t_1}^{t=t_2} \left| DEV1_i \right| \qquad \text{(Equ. 5)}$$

When considering the sign, also the direction of deviation reveals:

$$DEV2_i\_SIGN = \sum_{t=t_1}^{t=t_2} DEV1_i \qquad \text{(Equ.6)}$$

The averaging of the deviation DEV2 over all measurement positions leads to the average accumulated deviation DEV3_ABS and DEV3_SIGN. These values are absolute ones and are in same units as the mixing scalar [%]. The relative deviations $DEV3_{rel}$ are calculated relating the absolute deviation DEV3 to the integral perturbation introduced in the experiment into the core inlet plane.

Comparison for the stationary experiment ROCOM-stat01

Four CFD solutions obtained by different project partners were included into the comparison between measurement and calculation. Each project partner provided the solution calculated using the production mesh. The production mesh is the result of the application of the Best Practice Guidelines to the creation and qualification of the computation grid and the solutions. The details are included in D11 [3].

Besides the three steady state calculations, one transient calculation was included into the comparison (FZR_01_{tr}). This calculation was performed with constant velocity boundary conditions at the inlet into the reactor pressure vessel. The calculated mixing scalar at the core inlet was averaged at the quasi-stationary concentration level in the same way as in the experiment. The results of the four calculations are shown on fig. 21 (see section C.4.2).

Tab. V shows the relative averaged deviation DEV3 for the different CFD solutions. The averaged perturbation should be close to 25 % in the case of 100 % perturbation in one of the four loops. However, the exact value of the perturbation depends on the velocity profile at the core inlet, which is unknown, but should be close to homogeneous in our case. The relative deviation considering the sign is very low for all calculations in comparison to the absolute deviation. That indicates, that a tilt between the measured and the calculated distributions

leads to a significant compensation. The relative deviation based on the absolute values is in the order of 25 % for all solutions.

Quantitative comparisons are also performed for the experiments ROCOM-stat04 and ROCOM-stat09. FLUENT calculations have been performed for these experiments by VUJE and AEKI. The results are presented in D11 [3]. The tendencies are the same as observed for ROCOM-stat01.

Comparison for the slug mixing experiment ROCOM-02

Two solutions of FZR using the codes CFX-4 and CFX-5 were included into the comparison between measurement and calculation. Both calculations are obtained with the corresponding production mesh (tetrahedral mesh for CFX-5). In Tab. VI, the maximum values and the time point of maximum are compiled for the experiment and the two calculations. Both calculations predict the maximum of the mixing scalar slightly too early, 1 or 0.5 s respectively. The value calculated by CFX-4 of the maximum is in good agreement with the measured one, while being overestimated in the CFX-5 calculation. Further, the accumulated normalized perturbation PERT was calculated according to:

$$PERT = \frac{1}{(t_2 - t_1)} \sum_{t=t_1}^{t=t_2} \frac{1}{n} \sum_{i=1}^{n} \Theta_i(t) \qquad \text{(Equ. 7)}$$

The integral perturbation is normalised in this way, that a value of PERT0 = 1.0 would be reached, when the mixing scalar over the whole considered time would be unity at all measurement positions, with other words we would have a full deboration over the full considered time. The integral perturbation was 0.146 in the experiment, 0.1566 in the CFX-5 calculation and 0.1124 in the CFX-5 calculation. In the CFX-4 calculation the introduced perturbation was underestimated in comparison to the experiment, whereas the it was overestimated in the CFX-5 calculation.

Conclusions on quantitative comparison between measurement and CFD-calculations

A detailed quantitative comparison of the results of CFD-calculations with measurements in the complex geometry of the model of a pressure vessel was performed. Different steady-state and transient experiments and calculations were considered. The comparison was mainly concentrated on the core inlet plane. Additionally, the velocity distribution in the downcomer was compared.

In the steady state experiments, the different codes show the same global tendencies. The quantitative analysis revealed, that the spreading of the tracer in radial direction is underestimated in all presented calculations. The transient calculation with constant velocity in time shows the best agreement in the shape of the distribution of the mixing scalar in the core inlet plane and in the calculated maximum value. Further, the comparison of measurement positions, for which the coolant should flow through the sieve drum or around the sieve drum revealed great differences.

The pump start-up experiment ROCOM-02 was calculated by the codes CFX-4 und CFX-5. The time behaviour of the maximum and the average perturbation calculated by both codes is

inside the confidence interval of 2 σ during the main part of the considered time interval. The analysis of the different types of deviations used for the quantitative assessment, showed the general tendency that the CFX-4 solution is in better agreement with the experimental results. This is supported by the assessment of the single measurement positions: The calculated by CFX-4 maximum value at these positions as well as the calculated time of the maximum fits into the confidence intervals of the measurement results at more positions than the CFX-5 calculation.

The introduction of such a comparison allows to quantify the deviations of different calculations form the experimental results. The use of the obtained data contributes to the assessment of the quality of the calculations and give the possibility to create a ranking of the different calculations. A detailed quantitative assessment of the correspondence between measurement and calculation can support further code development activities.

C.4.5 CFD calculations for Vattenfall experiments

CFD calculations have been performed for the VATT-02 test case from the Vattenfall experiments (see table I). It is a slug mixing transient, with a slug with low boron concentration initially present in the RCS pipe. Buoyancy forces are negligible. The Vattenfall experiments are described in detail in the report of WP2 [1]. Calculations have been made by PSI (CFX-5 code), Vattenfall Utveckling and NRI (FLUENT).

Calculations were made with two different grids, "Grid 1" with 200,726 cells and "Grid 2" with 1,605,808 cells. Grid 1 is a quite coarse grid and is considered to have about the minimum number of cells required to get a fair resolution of the flow field. Grid 2 is a complete refinement of Grid 1, i.e. to get Grid 2 all cells in Grid 1 are split up into 8 cells. According to "the Best Practice Guidelines for CFD" grid refinements should be made in this way.

13 different turbulence models were tested, 6 versions of the RSM included.:

- RNG k-ε, Standard k-ε, Standard k-ε (Kato-Launder) and Realizable k-ε
- Standard k-ω and SST k-ω
- RSM, with the following versions: LRR-IP, QI, SSG, Omega, Omega (BSL)

RNG k-ε was treated as the first choice turbulence model. Most sensitivity tests for turbulence models were made only for steady state conditions. Steady state calculations were all made with Grid 1, the coarse grid, except for the RNG k-ε model. The differences in results between calculations with different turbulence models were quite big. The best result was achieved with the RNG k-ε model. Also for the slug mixing transient the RNG k-ε model gave the best agreement with experimental data, compared to the RSM (Omega BSL) and the k-ω SST model.

Comparisons with measurements are only made for the calculations that showed best agreement with measurements. These calculations have the following characteristics.

- Code: CFX5.6 (steady-state)and CFX5.7 (slug mixing)

- Grid: Grid 2 for slug mixing transient, Grid 1 for steady state (calculations with Grid 2 had convergence problems for the steady state situation, showing a periodically fluctuating velocity field with a higher frequency instability superimposed upon it)
- Turbulence model: RNG k-ε model

The mean and the minimum dimensionless boron concentrations (corresponding to unity minus mixing scalar) are quite well met in the FLUENT calculations for the VATT-02 slug mixing test. Figure 25 shows mean and minimum (independently on position) dimensionless boron concentrations at the core inlet as a function of time. The calculated minimum boron concentration for the Grid 2 calculation with the RNG k-ε model is very close to the measured value (see figure 25 right). This indicates that we are close to get a grid-independent solution. However, to be able to check this, one would have to make a calculation with a further refined grid (ideally with a grid with 8 times as many cells as Grid 2, i.e. around 13 million cells). A calculation with this grid is not possible to perform today, with the available computer resources.

The calculated concentration is, however, delayed around 0.9 s compared to the measured concentration. This can to a large extent be due to an inaccuracy in the measured flow rate.

However, not only the minimum boron concentration should be met well, but also the positions of low boron concentrations must be captured. Two "islands" of low boron concentrations are present in both the measurement and in the CFD calculation. However, the calculated minimum is positioned far from the measured minimum (Fig. 26). The displacement of the concentration field is mainly a rotational displacement. One reason for calculating incorrect boron concentrations at the core inlet can be that the calculated velocity field is wrong. This will have an effect on the mixing and transport of the boron concentration field. The reasons for the difficulties to get the right velocity field are at least partially due to the large impact of the inlet boundary conditions described section C.4.1 (see Fig. 19).

Conclusions

Comparisons with measurements show best agreement with measurements for a calculation with CFX 5.7, the RNG k-ε turbulence model and a grid of 1,605,808 cells. The minimum average boron concentration at the core inlet was captured very well by this calculation. Also the minimum boron concentration at the core inlet was quite well simulated. The distribution of low boron concentration across the core inlet plane was not, however, accurately modelled by the CFD calculation.

The reasons for not getting a better agreement with measurements can maybe be found among the following items:

- Too few computational cells. Sensitivity tests showed a big influence of number of grid cells. Due to limited computer resources it could not be shown that a grid of 1,605,808 cells gives a grid-independent solution. There are, however, indications that this grid is not far from giving a grid-independent solution in this case. Maybe a few million cells will be enough for getting a grid-independent solution.
- A too long time step might have been used. Due to limited computer resources time step sensitivity tests have not been made.
- Simplifications in geometry can be more important than expected. Chamfers, vertical cylinders and the lowest structure in the lower plenum are neglected. Even if these

structures are small they can have a significant influence on the flow field and the mixing. A sensitivity test showed that it is very important to model the horizontal structures in the lower plenum.

- Poor modelling of turbulence. Sensitivity tests showed big differences in results for different turbulence models, which indicates that more advanced turbulence models will give a better agreement with measurements. In the VATT-02 slug mixing transient there are certain features that are especially problematic for turbulence modelling, which also points to the need for more advanced turbulence models than have been used here. These are:
  - transition to turbulence in accelerating flow
  - impinging jet at the entrance to the downcomer
  - flow past obstructions

C.4.6 CFD calculations for the GIDROPRESS experiments

NRI simulated two from three slug-mixing experiments provided by EDO Gidropress (see section C.2.2). The experiments simulated slug mixing in the reactor vessel of a VVER-1000 reactor. In the tests, the experimental facility was filled with hot water (temperature of 71 °C in test 1, 73.3 °C in tests 2) and slug of cold water (temperature of 25.8 °C in test 1, 27.4 °C in tests 2) was situated in the loop seal. The loop flow rate was then increased up to 175 m^3/hr (test 1) and 470 m^3/hr (test 2).

In test No.1 the elliptical perforated bottom with original 1324 holes (diameter of 8 mm) was modelled as porous media zone in the first version of the grid (variant 1A), and the number of holes was decreased to 312 holes with diameter of 16 mm in the second grid (variant 1B). In test No.2 the elliptical perforated bottom was modelled with the reduced number of holes. View of the grid and calculation domain used in test 1 is shown on Fig. 27.

At walls, adiabatic (Neumann) boundary condition was used for the energy equation. For test 2, also adiabatic and constant temperature boundary conditions were tested (variant 2A and 2B). Realizable k-ε model was used with differential viscosity option and standard wall functions (y^+ lower than 250). Full buoyancy effects including the effect of buoyancy on ε were considered.

Fig. 28 shows the dimensionless averaged temperature at the core inlet. Calculated minimum of average core inlet temperature is lower than the experimental one. The calculated average values are almost independent from the grid option (porous body or reduced number of holes). Fig. C.4.41 shows the temperature distribution at the core inlet calculated with both grid options. Grid with perforated bottom (variant 1B) provides better mixing than grid with porous zone (variant 1A). The underestimation of the minimum value in the calculation is an indication, that heat exchange between cold slug and walls cannot be neglected.

Calculated cold slug lags behind the experimental one. The reason for this time shift could not be clarified finally.

The transient of the average dimensionless temperature at the core inlet for the test 2 is shown on Fig. 29. In variant 2A zero wall heat fluxes are assumed as in the simulations of tests 1. In

variant 2B, constant wall temperature, equal to temperature of the hot water outside the cold slug, is assumed. In both cases, detailed model of the perforated bottom and realizable k-epsilon model are used. In case 2A, no heat release from the wall to the fluid is considered. The minimum temperature is underestimated in the calculation. In the case of constant wall temperature, the heat release is overestimated, because in reality, the wall will be cooled down somewhat, which leads to a reduction of the heat flux. Consequently, the minimum temperature is overestimated in the calculation. In the case of realistic heat transfer modelling (solution of the coupled fluid dynamics – heat conduction problem), a good agreement between measurement and calculation can be expected. However, this coupled calculation could not be performed within the FLOMIX-R project.

C.4.7 CFD calculations for the buoyancy-driven mixing experiments

CFD simulations have also been performed for the buoyancy driven mixing tests. Three of the Fortum PTS and tests and one ROCOM generic buoyancy driven mixing case have been calculated.

CFX-5 calculations of the buoyancy mixing test D10M05 were performed by GRS. The experiment was performed with injection of water with 10 % increased density into the cold leg with 5 % of nominal flow rate. The calculational grid provided by FZR includes detailed models of the sieve barrel, the core support plate and the rods modelling the core in the ROCOM test facility. The cold leg with the ECC-injection nozzle was added in order to capture the flow stratification in the cold leg which also influences mixing in the downcomer. The injection of water with higher density was performed from 5 – 15 s. Calculations were made using second order discretisation schemes in space and time. Two constant time steps (0.1 sec and 0.05 sec) were used in combination with the SST turbulence model and scalable wall functions. Fig. 30 (upper) shows the flow in the cold leg during and after the injection of the glucose solution. There is a strong stratification with a higher concentration of glucose on the bottom of the cold leg. The glucose solution flows downwards directly below the inlet pipe (see Fig. 30, lower). These phenomena were also observed in the experiment.

Investigations on the influence of the turbulence model were performed by using a Reynolds Stress model (RST), based on the omega equation. The RST model, although calculated with the larger time step (due to higher computer resources requirements), shows better agreement with measurement data (see e.g. Fig. 31).

However, quantitative comparison between measurement and calculation is difficult especially for the buoyancy driven mixing cases because of the fluctuating nature of the flow field and mixing pattern. It might be more useful to compare some averaged or integral parameters. This was done e.g. for the Fortum PTS experiments.

The buoyancy driven turbulent flow with stratification and mixing in selected Fortum mixing tests was modelled with the commercial CFD code FLUENT. The comparison was mainly based on the temperature/concentration data from the thermocouple locations near the pressure vessel wall and in the main (middle one) cold leg. The stratification and mixing in the main loop was studied using backflow ratio $Q^* = Q_h/Q_{HPI}$ where Q_{HPI} is the cold-water injection flow rate and Q_h is the flow rate from the downcomer to the main loop. The mixing

of the cold water plume in the downcomer was studied using time-dependent maximum and average injection water concentrations at RPV wall at different vertical levels.

Fig. 32 shows a comparison of the measured and calculated the backflow ratio (left) and the maximum concentration of the cold HPI water in the downcomer. The main features of flow and mixing were quite well simulated; stratification in the main cold leg and the downcomer, backflow from the downcomer and side loops to the main loops and the flow field in the downcomer. However, the mixing of the cold water plume was not as effective in simulations as in real experiments. More grid size tests with transient simulations are needed to test the grid-independency of simulations, the steady state tests made in this work are not good enough due to the poor convergence. Preliminary turbulence models tests with Realizable k-ε (Fortum 10.1) and RNG k-ε models (NRI 10.3) did not bring out any significant differences between models. The calculation with RNG k-ε model was performed by the project partner NRI Řež (Czech Republic).

C.4.8 CFD simulation mixing tests at Paks NPP (VVER-440 reactor)

Additional test data were made available by Paks NPP and AEKI for the FLOMIX-R project. The data come from the commissioning tests of Paks NPP performed in years 1987-1989. The tests addressed mixing among coolant loop flows in the downcomer and up to the core inlet in forced flow conditions. The goal of the tests was investigation of potential loop temperature asymmetry that might occur and significantly affect power distribution in the core. An overview on the results is given in Section C.3.3. Detailed description of the tests can be found in reference [18]. Paks mixing experiments were calculated by VUJE (FLUENT), AEKI (FLUENT) and TU Budapest (CFX5).. More detailed Descriptions of the CFD analyses is given in D11 [3].

Comprehensive computer models of VVER 440 reactor vessel were developed. They include all 6 loops with inlet nozzles and three baffles, whose purpose is to deflect the coolant injected into the reactor vessel from the safety injection tanks. Eight support consoles for the core barrel alignment were modelled as well. An overview on the different geometrical models is given in table VII. The production mesh of VUJE is shown on Fig. 33.

The sensitivity tests of the meshing showed that the calculation meshes did not meet the grid-independency criteria, in spite of the large node number. It was concluded that hybrid tetrahedral-hexahedral mesh seems to be more suitable for the meshing of the pressure vessel geometry because of the lower mesh element number (in the new versions of the CFX hybrid meshes are available.)

Comparison of the calculation results with the measurements was done only for that simulations which gave the best agreement (“production calculations”). Summary of basic assumptions used in the production calculations of Paks mixing tests performed by AEKI, TU Budapest and VUJE is presented in Table VIII. All calculations were performed as steady-state.

Results are shown in Fig. 34 in the form of temperature fields expressed in terms of mixing scalars at the core inlet and compared with experimental data. For assessment of deviations between calculated results and measurements, maps of errors are presented as well.
The performed calculations showed that the coolant flows in sectors downwards in the downcomer, and the sectors remain also at the core inlet. The maximum of the mixing scalar is not located directly below the inlet nozzle, but an azimuthal shift of the maximums can be observed because of the asymmetric location of the inlet nozzles and because of the hydro-accumulator baffles. The effect of the baffles can be observed even at the core inlet.

The sensitivity tests of the meshing showed that the calculation meshes did not meet the grid-independency criteria, in spite of the large node number. It was concluded that hybrid tetrahedral-hexahedral mesh seems to be more suitable for the meshing of the pressure vessel geometry because of the lower mesh element number (in the new versions of the CFX hybrid meshes are available.)

Summary and conclusions from VVER mixing tests calculations
The results show qualitatively good accordance with the measured data. However, the mixing is underestimated in the calculations (the calculated maximums of the mixing scalars are larger than the measured ones).

- Good numerical convergence was achieved with basic solver and solver settings based on residuals of continuity and momentum equations (using first order upwind discretization scheme and k-ε or RSM turbulence model).
- Some numerical fluctuations of the flow field were observed below the ECC baffles in the downcomer, possibly due to some non-stationarity of the flow field.
- Modelling of detailed internal geometry (e.g. flow baffles) may have a noticeable influence on results.
- ECC water baffles guide the main flow and generate turbulence effects in the downcomer.
- The alignment drifts have only local effect.
- Accurate model of the perforated elliptical bottom (modelling the elliptical perforated bottom as solid structure rather than using a porous medium) provides more realistic flow pattern and improves the accuracy of the calculation.
- The models should include the upper plenum and the outlet nozzles.
- Using pressure outlet boundary condition gives better numerical convergence than outflow boundary.
- Boundary layer at the walls of downcomer should be less then 3mm, to keep y^+ parameter less then 1000.
- High order methods decrease the stability of the solution.

C.4.9 Summary and conclusions from CFD code validation

The purpose of FLOMIX-R WP4 was to obtain indications on how well boron dilution transients and steady state mixing in Pressurized Water Reactors (PWR) can be modelled by CFD codes and to give recommendations for use of CFD for these purposes. CFD calculations have been validated against measurements from four different test facilities. In this section, a summary of the conclusions and recommendations made from these calculations are given and also discuss what needs to be done to strengthen the CFD tool for turbulent mixing applications are discussed.

C.4.9.1 Conclusions from sensitivity tests according to the BPG

The most important conclusions from the sensitivity tests made in WP4 and WP3 are presented below. Sensitivity tests are an important part of applying the Best Practice Guidelines for CFD in terms of quality assurance. Sensitivity tests will tell if you have a grid- and timestep-independent solution, or if results are sensitive to inlet and outlet boundary conditions, modelling of geometry and turbulence model etc. As the test facilities for which the validations were made are quite different, it is in some cases difficult to draw general conclusions. The conclusions are also based on calculations that have not been shown to be grid independent.

Grid size

The aim is to make CFD calculations that give grid-independent solutions, i.e. results that do not change when the grid is refined further. A grid-independent solution can be defined as a solution that has a solution error that is within a range that can be accepted by the end-user, in view of the purpose of the calculations. According to the BPG, calculations must be made with at least three different grids in order to be able to quantify the grid-dependence of the calculations. The two finer grids also have to be made using a complete refinement of the nearest coarser grid, to get an objective measure of the grid-dependency. For example, if a calculation is made with 200,000 cells, calculations also have to be made with 1,600,000 cells and 12,800,000 cells. Due to limited computer resources, this procedure has not been possible to follow for any of the slug mixing test cases in FLOMIX-R WP4. A transient calculation for a coarse grid of around 200,000 cells takes in the order of one week to perform. The solution errors have therefore not been quantified. Developments in computer technology will make these quantifications of solution errors possible within a few years. The number of cells required for grid-independency can only be guessed. Several million cells are probably needed for most of the transient test cases in FLOMIX-R. In spite of fully grid-independent solutions, solutions on so-called production meshes were used to assess the agreement between measurement and calculations. The production meshes were an optimum in mesh refinement what could be reached.

Inlet boundary position and inlet boundary condition

It is well known that the choice of inlet boundary position and inlet boundary condition (turbulence level, variation in inlet velocity field in space and time) can have a big influence on the flow pattern far downstream from the inlet. Some partners therefore made sensitivity tests; others put the inlet far upstream from the downcomer at a position where the flow conditions were well known.

For the ROCOM steady state mixing case, results were not sensitive to different turbulence intensities at an inlet positioned close to the downcomer. Slightly different results were

achieved if the concentration profile was changed at the same inlet position. Modelling of the four cold legs, bends included, gave only slightly different results compared to having an inlet close to the downcomer.

Outlet boundary position and outlet boundary condition

For the Vattenfall steady state flow situation the results were only slightly sensitive to whether the main outlet was put at the core inlet or at the core outlet. For the ROCOM cases it was found that the main outlet should be put above the core inlet.

Modelling of internal geometry

Internal structures can have a big influence on flow and mixing. These structures can either be omitted, be simplified or be modelled in detail. One type of simplifying model is a porous media model, with distributed resistances. Especially how the structures in the lower plenum are modelled can have a big influence on flow and mixing. There were different experiences concerning the importance of modelling the lower plenum structures. These are listed below. For most applications, a detailed model gave results that were in best agreement with measurements. A general recommendation should be that internal structures should be modelled in detail. One should be very careful with decisions to omit these structures or to use simple forms of the porous media approach.

For the ROCOM steady state calculations using CFX4, a porous body model of the steel plate and sieve barrel gave reasonably good results. For the calculations with CFX5, however, detailed models of these structures gave better agreement with measurements than using a porous media model. Also for the NPP PAKS and GIDROPRESS calculations, detailed modelling of this types of structures gave better agreement with measurements. For the Vattenfall steady state case, inclusion of the lower plenum structures has a significant positive influence on the flow field in the downcomer. For the FORTUM PTS tests, modelling of the bottom plate only had a small influence on the flow field.

Turbulence models

For the Vattenfall slug-mixing transient the best results were achieved with the RNG k-ε model, with scalable wall functions, compared with the k-ω SST model and the RSM (Omega (BSL)), with automatic wall functions. For the ROCOM transient buoyant case, RSM (BSL) gave improved results compared to the Standard k-ε and the k-ω SST model. For the ROCOM steady state mixing and non-buoyant transient mixing, the results were not very sensitive to turbulence model (the Standard k-ε model and the k-ω SST model gave similar results). For the (buoyant) FORTUM PTS tests, the Realizable k-ε model produced better results than the RNG k-ε model. For the VVER mixing test calculations the Standard k-ε model with non-equilibrium wall functions and RSM with standard wall functions gave the best agreement. RSM with non-equilibrium wall functions and the k-ω SST model overestimated the mixing.

The conclusions presented above are in some cases contradictory. The RSM models should give better agreement with measurement, as they are more advanced than the two-equation models. This was not always the case for the calculations in FLOMIX-R. The contradictory conclusions make it hard to draw any general conclusion on which turbulence model to use. It should, however, once again be emphasized that these results are based on calculations that have not been shown to be grid-independent.

In general, standard turbulence models implemented in the codes can be used for turbulent mixing calculations.

Double precision
In general, the use of double precision arithmetic is recommended, but it requires more computer resources. Single precision arithmetic was used only if it was not shown that single precision gave identical results to using double precision for a similar case.

Time step
Especially if the CFL number (the Courant-Friedrichs-Lewy number) is larger than 1, and especially where there are strong gradients, one can expect problems with time-step dependency. For the sensitivity tests made for time-step, time-step independency was reached with time steps which were as long as up to 10 times the CFL number (FORTUM PTS) and 50 times the CFL number (ROCOM slug mixing transient). These CFL number are for positions where there are large gradients in concentration or temperature.

Height of wall-adjacent cells
One sensitivity test was made for the height of the wall-adjacent cells for the Vattenfall steady state case. The maximum y^+ values were very high with the grids used, up to around 5000. The grid was therefore refined at the wall-adjacent cells. However, calculations with these lower and more optimum y^+ at the walls gave worse results for the Vattenfall steady state case. This might indicate that the non-equilibrium wall function used does not work properly for the type of boundary layers present in the downcomer, especially those close to the flow-impingement where the jet from the inlet pipe hits the downcomer wall. For the ROCOM production mesh the y+ value in the downcomer was 65, and therefore below the recommended value of 100.

Code
The commercial codes CFX4, CFX5 and Fluent 6 were used. For both the Vattenfall slug mixing case and the ROCOM_02 slug mixing case the differences between the results from Fluent 6 and CFX5 were significant, in spite of the fact that the calculations were run with exactly the same grids. For the ROCOM steady state mixing case, the differences were smaller.

However, as none of the calculations are probably grid-independent, one cannot expect to obtain the same results from the codes, as the numerics in the codes are different. Another difference between the two codes is that exactly the same wall functions could not be applied.

Numerical schemes
At least second order schemes should be used, both in space and time. For some applications there were convergence problems (unstable solutions) when using 2^{nd} order schemes. This might indicate that there are also low-frequency fluctuations in the measurements, which cannot be resolved by a steady-state calculation. For these cases a time-averaged flow field might have to be calculated with a transient calculation.

C.4.9.2 Comparisons with measurements

Steady-state mixing and flow distribution
In general, the flow pattern, velocity distribution in the downcomer and mixing scalar distributions at the core inlet are well predicted in the CFD calculations. The velocity field in the downcomer has inhomogeneous character with maximum downwards flow components in the regions in-between the inlet nozzles. A clear sector formation of the flow in the

downcomer is seen. This leads to maximum mixing scalar values at the core inlet of 92 – 99 %. That means, a part of the fluid remains almost unmixed. The re-distribution of the velocity field and mixing scalar distribution in the case of asymmetric flow conditions is also qualitatively well reproduced in the calculations.

Finer grids in the CFD simulation tend to give better results. Also modelling of perforated sheets (such as the drum in the downcomer) as real structure rather than porous medium improves quality of results. Influence of porous medium as a substitute of a perforated sheet can be, in some extent, controlled by proper definition of direction-dependent resistance of the porous medium. Other investigated effects (turbulence model, wall function, position of outlet boundary) do not have an unambiguous influence on results. In general, the mixing along the flow path in the downcomer is under-predicted in all calculations. Disturbance in the inlet boundary conditions has significant impact on the flow pattern. This can be seen in experiment ROCOM-stat01, where a disturbance in turbulence or swirl intensity caused by the mixer is assumed to be responsible for an observed perturbation in the velocity distribution.

Slug mixing transients

For the ROCOM slug-mixing transient the qualitative agreement with measurements is good. The position of the lowest boron concentrations was captured fairly well. Quantitative good agreement with the level of the measured lowest boron concentrations was achieved. Considering the agreement of the measured and calculated boron concentration values at local positions, the deviations are larger than for the global minimum. For the ROCOM buoyant slug mixing transient, the local concentration was over-predicted, i.e. mixing was under-predicted.

For the Vattenfall slug-mixing transient, the minimum average boron concentration at the core inlet was captured very well by the CFD calculations. Also, the minimum boron concentration at the core inlet was captured very well. The distribution of low boron concentration across the core inlet plane was not, however, accurately modelled by the CFD calculation. The calculated position of the minimum concentration was found around 0.52R from the measured position of the minimum concentration (where R is the radius of the core inlet plane). The displacement of the concentration field is however mainly a rotational displacement. The difference in radial position of the minima is only about 0.15R. This could be relevant in reality, as a core is primarily different radially, as far as enrichment and reactivity are concerned. The results with the best agreement with measurement data were obtained using CFX-5. However, comprehensive studies were performed by Vattenfall using the FLUENT code. They are reported about in Annex 6 of [D11].

In the GIDROPRESS slug mixing transient the calculated minimum of the average core inlet temperature was lower than the experimental one. This was probably a consequence of the fact that the heat exchange between the cold slug and the warm walls was neglected in the CFD calculation. Other possible reasons are the pre-mixing in the main coolant pump simulator, which is difficult to model, and the not exactly known initial position of the slug boundary.

The CFD calculations for the FORTUM PTS buoyant transient mixing case modelled the main features of the flow quite well. Quantitatively there was some poor agreement for mixing in the main loop and for the mixing of the cold plume in the downcomer.

The conclusions from the various calculations made were not unanimous. The results are promising, however, better agreement with measurements is needed for a CFD calculation to be an equivalent competitor to model tests. The continuous developments in computer capacity and in software capabilities will allow more extensive calculations to be made, enabling a reduction in errors from all sources, and increase the accuracy of CFD calculations. A methodology of quantitative comparison between measurement and calculation was developed and applied. It provided very useful information concerning a quantified engineering error assessment which can be used e.g. in reactor physics calculations concerning the consequences of boron dilution transients as a safety surcharge.

C.4.9.3 Development needs

This section gives a summary of the conclusions drawn from the WP4 and WP3 calculations concerning what is needed in the future to obtain more accurate CFD calculations for boron dilution transients and mixing in Pressurized Water Reactors. As shown earlier in this report agreement with measurements is not satisfactory in most cases. In order to get results from CFD calculations that are in better agreement with measurements, the following points have to be considered:

- More computational cells. No grid-independent solutions were presented in FLOMIX-R WP3 and WP4. More detailed modelling of internal structures might also be needed, which leads to additional cells.
- Shorter time-steps might in some cases be needed
- More advanced turbulence models, especially models that can cope with the specific features of the flow fields present in these applications, such as accelerating flow, flow-impingements and buoyancy. Further-improved Reynolds Stress Models or LES models (or hybrids between the two) might be needed to get better agreement with measurements. Better models of wall boundary layers (i.e. wall functions) are also probably needed.
- Some steady state cases have to be run as transients, as low-frequency fluctuations cannot be captured by a steady-state calculation. A transient calculation takes at least an order of magnitude longer time to perform than the corresponding steady-state calculation.

The computation time needed for a grid- and time step-independent CFD calculation using an advanced turbulence model is today too long (in the order of months). To be able to perform such calculations in a shorter period of time, the following aspects are important:

- Faster computers
- Faster and more accurate solvers and numerical schemes
- Lower costs for parallel licenses of CFD codes. Today, parallel license costs are higher than costs for hardware.

- Automatic time-stepping. The CFD code should choose the optimal time-step (within specified limits) and relaxation for minimizing computation time and ensuring convergence to specified residual levels.
- Improvements of the grid generation process in order to be able to, in an easier way than today, make high-quality hexahedral grids that would produce more accurate solutions with fewer cells.
- Grid adaptation (refine & coarsen) during transient runs to get refinements where there are strong gradients of (especially) concentration will also produce more accurate solutions with fewer cells.
- Refined porosity models can reduce the need for cells.

The Best Practice Guidelines for CFD have increased the awareness for what is needed to produce high-quality CFD calculations. These guidelines should be extended with more detailed recommendations, for example which turbulence model to use for different types of flow situations. The CFD code should also help the user to apply the Best Practice Guidelines, for example concerning quality checks for grid and solution.

More general conclusions, encompassing more scenarios relevant for nuclear power safety, are presented in the reports from the ECORA Project.

In spite of the large amount of work performed in FLOMIX-R there are still questions unanswered about the capability of CFD codes to model boron dilution transients and mixing in primary system in Pressurized Water Reactors (PWR). The continuous development in computer capacity and in software capabilities will continuously increase the ability to make accurate CFD calculations.

In general, it can be concluded, that CFD codes can be applied for calculations of turbulent mixing in one-phase flow in an engineering way.

D. Conclusion

A new quality of research in flow distribution and turbulent mixing inside the RPV of nuclear reactors has been achieved in the FLOMIX-R project. Experimental data on slug mixing with enhanced resolution in space and time have been gained from various test facilities covering different geometrical and flow conditions. The basic understanding of momentum controlled mixing in highly turbulent flow and buoyancy driven mixing in the case of relevant density differences between the mixing fluids has been improved significantly. An unique data base has been created for the CFD code validation for turbulent mixing applications in nuclear reactor safety analysis.

In WP1, the key mixing and flow distribution phenomena relevant for both safety analysis, particularly in steam line break and boron dilution scenarios, and for economical operation and the structural integrity have been identified. Based on this analysis, test matrices for the experiments are elaborated, guidelines for the documentation of the measurement data and for performing validation calculations with CFD codes are provided.

In WP 2 on slug mixing tests, experiments on slug mixing at the ROCOM and Vattenfall test facilities were performed. The measurement data were made available to the project partners for CFD code validation purposes. Additional slug mixing tests at the VVER-1000 facility of EDO Gidropress were made available. Two experiments on density driven mixing (one from ROCOM, one from the Fortum PTS facility) were selected for benchmarking.

In WP 3 on flow distribution in the cold legs and pressure vessel of the primary circuit, commissioning test measurements performed at the Paks VVER-440 NPP were used for the estimation of thermal mixing of cooling loop flows in the downcomer and lower plenum of the pressure vessel. A series of quasi steady state mixing experiments was performed at the ROCOM test facility. CFD methods were used for the simulation of the flow field in the primary circuit of operating real scale reactor. Computed results were compared to available measurement data, and conclusions are drawn concerning the usability and modelling requirements of CFD methods for that kind of application.

In WP 4 on validation of CFD codes, the strategy of code validation based on the Best Practice Guidelines was defined. A matrix of CFD code validation calculations was elaborated. CFD validation calculations on selected benchmark tests were performed. The CFD validation work was shared among the partners systematically based on the validation matrix. Systematic studies have been performed concerning the sensitivity of the calculated results from meshing, time step, boundary conditions, turbulence models and their model parameters. Optimum modelling options have been identified for the different applications. A methodology of quantitative comparison between measurement and calculation was developed and applied. It provided very useful information concerning a quantified engineering error assessment which can be used e.g. in reactor physics calculations concerning the consequences of boron dilution transients as a safety surcharge.

The experience gained in the project will increase the competitiveness of the European research and engineering support organisations as well as nuclear electricity generating industry. Research and engineering organisations involved in the project are Serco Assurance, GRS, PSI and FZR. The project partners Fortum Nuclear Services and Vattenfall Utveckling are important representatives of European nuclear industries. The participation of the European higher education establishments in the project supports the education of nuclear experts. A number of students and PhD students was involved into the work. The NAS extension of the project was focused to VVER type reactors and was performed by partners from VVER operating countries, which were newly associated to the EU and now are EU member states. It will help to harmonise safety assessment approaches and to reach comparable level of understanding the relevant phenomena. A VVER nuclear power plant (NPP Paks) as well as organisations providing technical support for NPPs and nuclear authorities (VUJE Trnava, NRI Rez, AEKI Budapest) were participating in FLOMIX-R The general designer of VVER type reactors, Experimental and Design Organisation “Gidropress”, was involved. Quality assurance practice for CFD was applied based on the ERCOFTAC BPG specified in the ECORA project for reactor safety analysis applications. Serco Assurance and Vattenfall experts are active in the ERCOFTAC. Most of the FLOMIX-R project partners were participating also in ECORA aimed at an assessment of CFD methods for reactor safety analyses. FLOMIX-R is contributing to the extension of the experimental data base on mixing and CFD applications to mixing problems. Recommendations on the use of CFD codes for turbulent mixing problems gained in FLOMIX-R were fed back to the ECORA and ERCOFTAC BPG.

References

[1] S. Kliem, U. Rohde, B. Hemström et al.: "Description of the slug mixing and buoyancy related experiments at the different test facilities (Final report on WP2)", EU/FP5 FLOMIX-R report, FLOMIX-R-D09, FZ Rossendorf (Germany), October 2004

[2] Toppila, T., Hemström, B., et al., Flow distribution in the primary circuit (Final report on WP 3), FLOMIX-R-D10, Fortum Nuclear Servives, Espoo (Finland), 2004

[3] Hemström, B., et al., Validation of CFD codes based on mixing experiments (Final report on WP4), EU/FP5 FLOMIX-R report, FLOMIX-R-D11, Vattenfall Utveckling (Sweden), 2005

[4] Rohde, U. et al. : "Fluid mixing and flow distribution in the reactor circuit – measurement data base", Nuclear Engineering and Design 235 (2005) 421-443

[5] Rohde, U., Kliem, S., Toppila, T., Hemström, B., et al., Identification of mixing and flow distribution key phenomena, EU/FP5 FLOMIX-R report, FLOMIX-R-D02, FZ Rossendorf, Germany, 2002

[6] Final Report EUBORA – Concerted Action on Boron Dilution Experiments, Report AMM EUBORA(99) – P002, compiled by Harri Tuomisto, CEC, December 1999

[7] Grundmann, U.; Rohde, U. (1994): "Investigations on a Boron Dilution Accident for a VVER-440 Type Reactor by the Help of the Code DYN3D", Proc. ANS Topical Meeting on Advances in Reactor Physics: Reactor Physics Faces the 21st Century, Knoxville (Tennessee), 11. - 15. April 1994, Vol. 3, pp. 464 – 471

[8] Kliem, S.; U. Rohde, F.-P. Weiß (2004): „Core response of a PWR to a slug of under-borated water", Nucl. Eng. and Design 230, 121-132

[9] Rohde, U.; Elkin, I.; Kalinenko, V. (1997): "Analysis of a boron dilution accident for WWER-440 combining the use of the codes DYN3D and SiTAP", Nuclear Eng. and Design 170, pp. 95 – 99

[10] Kliem, S.; Höhne, T.; Rohde, U.; Weiß, F.-P. (1999): "Main Steam Line Break Analysis of a VVER-440 Reactor Using the Coupled Thermohydraulics System/3D-Neutron Kinetics Code DYN3D/ATHLET in Combination with the CFD Code CFX-4", Ninth International Topical Meeting on Nuclear Reactor Thermal Hydraulics (NURETH-9) San Francisco, California, October 3 - 8, 1999

[11] H.-M. Prasser, G. Grunwald, T. Höhne, S. Kliem, U. Rohde, F.-P. Weiss, Coolant mixing in a Pressurized Water Reactor: Deboration Transients, Steam-Line Breaks, and Emergency Core Cooling Injection, Nuclear Technology 143 (1), p.37, 2003

[12] H.-M. Prasser, A. Böttger, J. Zschau, "A New Electrode-Mesh Tomograph for Gas Liquid Flows," Flow Measurement and Instrumentation, 9, 111-119 (1998).

[13] Prasser, H.-M.; Zschau, J.; Peters, D. et al.:" Fast wire-mesh sensors for gas-liquid flows - visualisation with up to 10 000 frames per second", Int. Congress on Advanced Nuclear Power Plants (ICAPP), June 9-13, 2002 - Hollywood Florida, USA, Proc. CD-ROM, paper #1055

[14] Alavyoon, F., Hemström, B., Andersson, N. G., Karlsson; R. I.: "Experimental and Computational Approach to Investigating Rapid Boron Dilution Transients in PWRs," CSNI Specialist Meeting on Boron Dilution Reactivity Transients, State College, PA, USA, October 18-20, (1995).

[15] Logvinov S.A., Ulyanovsky V.N., Bezrukov Yu.A., Kozlov A.N.: " Mixing of coolant with different boron concentration at the VVER-1000 core inlet during RCP start-up", Proceedings of ANNUAL MEETING ON NUCLEAR TECHNOLOGY 2000, Bonn, 22-24 May 2000.

[16] Tuomisto, H.: "Thermal-hydraulics of the Loviisa reactor pressure vessel overcooling transients", Imatran Voima Oy, Research report IVO-A-01/87, 1987.

[17] Tsimbalov, S., et al. (1982), Coolant temperature distribution at VVER-440 core inlet. Atomnaya Energiya 52 (5), 304-308

[18] Elter, J., Experiment summary report, experimental investigation of thermal mixing phenomena in a six loop VVER type reactor, Paks Nuclear Power Plant Ltd, Safety Assessment Group, Flomix-R project February 2002

[19] CFX-4.4 Flow Solver User Guide, AEA Technology, 2001

[20] CFX-5.7 User Documentation, ANSYS-CFX, 2004

[21] FLUENT Inc., see http://www.fluent.com/

[22] FLUENT 6.1 user's guide, FLUENT Inc., 2003

[23] Casey, M. and Wintergerste T., "Best Practice Guidelines", ERCOFTAC Special Interest Group on Quality and Trust in Industrial CFD, Report, 2000.

[24] ERCOFTAC Best Practice Guidelines, see http://www.ercoftac.org/

[25] Menter F. et al. "CFD Best Practice Guidelines for CFD Code Validation for Reactor Safety Applications". Deliverable D01 of the EC project ECORA, 2002.

[26] Ulrych, G., Weber, E., Neuere Ergebnisse zur Kühlmittelströmung in Druckwasserreaktoren, Atomkernenergie-Kerntechnik 42 4, 217-223.

[27] S. Kliem, U. Rohde, T. Höhne, Data sets of the 1/5-scale slug mixing experiments at ROCOM facility, EU/FP5 FLOMIX-R report, FLOMIX-R-D05, FZ Rossendorf (Germany), 2003, incl.CDROM

[28] B. Hemström: Data sets of the 1/5-scale slug mixing experiments at Vattenfall facility, EU/FP5 FLOMIX-R report, FLOMIX-R-D06, Vattenfall Utveckling, Älvkarleby (Sweden), 2004, incl. CDROM

[29] S. Kliem, U. Rohde, T. Höhne (2003), Data sets on steady state mixing experiments at ROCOM facility, EU/FP5 FLOMIX-R report, FLOMIX-R-D07, FZ Rossendorf (Germany), 2003, incl.CDROM

[30] Y. Bezrukov et al., Documentation of slug mixing experiments of OKB Gidropress, EU/FP5 FLOMIX-R-D16, Podolsk (Russia), 2002

Table I
Matrix of sug mixing tests performed at the ROCOM and Vattenfall mixing test facitities

Run	**Ramp length [s]**	**Final volume flow rate [m^3/h]**	**Slug volume [m^3]***	**Initial slug position [m]***	**Status of unaffected loops**
ROCOM-01	14	185.0	40.0	10.0	Open
ROCOM-02	14	185.0	20.0	10.0	Open
ROCOM-03	14	185.0	4.0	10.0	Open
ROCOM-04	14	185.0	4.0	2.5	Open
ROCOM-05	14	185.0	4.0	22.5	Open
ROCOM-06	14	185.0	4.0	40.0	Open
ROCOM-07	14	185.0	20.0	10.0	Closed
ROCOM-08	28	92.5	4.0	10.0	Open
ROCOM-09	56	46.3	4.0	10.0	Open
ROCOM-10	14	148.0	4.0	10.0	Open
ROCOM-11	14	222.0	4.0	10.0	Open
ROCOM-12	14	185.0	8.0	10.0	Open
VATT-01	16	429	14.0	10.0	Open
VATT-02	16	429	8.0	10.0	Open
VATT-03	16	429	4.5	10.0	Open
VATT-04	40	172.8	8.0	10.0	Open

* related to the original reactor

Table II
Main features and parameters of the ROCOM and Fortum PTS test facilities with respect to buoyancy driven mixing

Feature	**Fortum PTS facility**	**ROCOM facility**
Measurement principle	Temperature	Conductivity
Density differences created by	Temperature (0.022) and salinity (up to 0.16)	Glucose solution (0.02 – 0.10)
Scaling	1:2.56	1:5
HPI	From bottom; Q_{HPI} = 0.1 – 4.0 l/s	From side: Q_{HPI} = 0.2 – 1.4 l/s
Flow rate in cold leg	Q_{CL} = 0 – 1.87 l/s	Q_{CL} = 0 – 12.8 l/s
Flow rate in adjacent loops	Q_{adj} = 0 – 2.0 l/s	Q_{adj} = 0

Table III
Selected ROCOM and Fortum PTS tests on buoyancy driven mixing with comparable boundary conditions

Nr	Q_{CL}(l/s)	Q_{HPI} (l/s)	$\Delta\rho_{HPI}/\rho$
Fortum PTS tests			
3	1.87	2.31	0.02
8	1.87	2.00	0.16
9	0	2.02	0.16
10	0	2.31	0.16
12	0	0.62	0.16
14	0.62	0.62	0.16
16	0	0.31	0.16
44; 45; 46	0	4.00	0.10; 0.16; 0.02
50	1.87	1.87	0.02
51	0	2.31	0.02
52	1.87	0.62	0.02
ROCOM buoyancy mixing tests			
3 - 8	7.72	1.00	0; 0.02; 0.03; 0.04; 0.05; 0.10
12 - 17	5.14	1.00	0; 0.02; 0.03; 0.04; 0.05; 0.10
26 - 31	2.72	1.00	0; 0.02; 0.03; 0.04; 0.05; 0.10
38, 39	0	1.00	0.05; 0.10

Table IV: ROCOM test matrix of steady state mixing experiments

Run ROCOM-stat	**Flow rate [m^3/h]**			
	Loop 1	**Loop 2**	**Loop 3**	**Loop 4**
01	185	185	185	185
02	50	50	50	50
03	185	back flow	back flow	back flow
04	185	185	185	back flow
05	185	back flow	185	back flow
06	185	185	back flow	back flow
07	185	back flow	back flow	185
08	203,5	166,5	185	185
09	222	148	185	185

The loop with the tracer solution injection in the test matrix is the loop number one.

Table V
Quantitative deviations between measuremnt and calculation for the test case ROCOM-stat01

	Averaged perturbation [%]	**DEV3_SIGN$_{rel}$ Equ. C.4.7 [%]**	**DEV3_ABS$_{rel}$ Equ. C.4.6 [%]**
EXP	25.45	-	-
FZR	25.40	-0.345	26.1
AEKI	24.95	-2.046	28.5
VUJE	25.26	-0.906	25.1
FZRtr	24.53	-3.810	24.4

Table VI
Measured and calculated maximum values of the mixing scalar
(including time of appearance)

	Total maximum [%]	**Time of total maximum [s]**	**Maximum of the average [%]**	**Time of maximum of the average [s]**
EXP	57.54	15.95	38.22	16.55
CFX5	60.34	14.50	33.12	17.00
CFX4	57.50	14.90	34.55	17.10

Table VII
Overview on geometrical modelling of the NPP Paks VVER-440

	VUJE	AEKI	TU Budapest
Loops	6	6	6
Baffles	simplified geometry	simplified geometry	Detailed geometry with gap between baffles and inner wall of downcomer
Alignment drifts	simplified geometry	simplified geometry	Detailed geometry
Elliptical perforated plate	Porous medium/ structure with reduced number of holes	Porous medium with direction dependent resistance (varied)	Momentum sources determined from calculations with reduced number of holes
Planar perforated plate	Porous medium	Porous medium	Lower plenum as porous medium with directed momentum source
Lower guide tubes	Simplified geometry of perforation/ omitted	omitted	
Core support plate	Porous jump/omitted	Porous medium	
Core	Porous medium/ omitted	Porous medium	Momentum sources/ omitted
Not modelled	ECC inlet nozzles; small structures, protrusions and chamfers	Lower guide tubes; ECC inlet nozzles; small structures, protrusions and chamfers	Lower guide tubes; ECC inlet nozzles; small structures, protrusions and chamfers

Table VIII: Basic assumptions used in the calculations of Paks mixing tests

	AEKI	TU Budapest	VUJE
CFD code used	FLUENT 6.1.22	CFX 5.5.1	FLUENT 6.1.18
Mesh	1 172 618	1 838 991	1 609 231
Elliptical perforated plate	Porous medium	Porous medium	Structure with 227 holes
Guide tubes	No	No	Yes (with perforations)
Discretisation scheme	1st order	2nd order	2nd order
Wall function	Non-equilibrium	Scalable	Standard

FIGURES

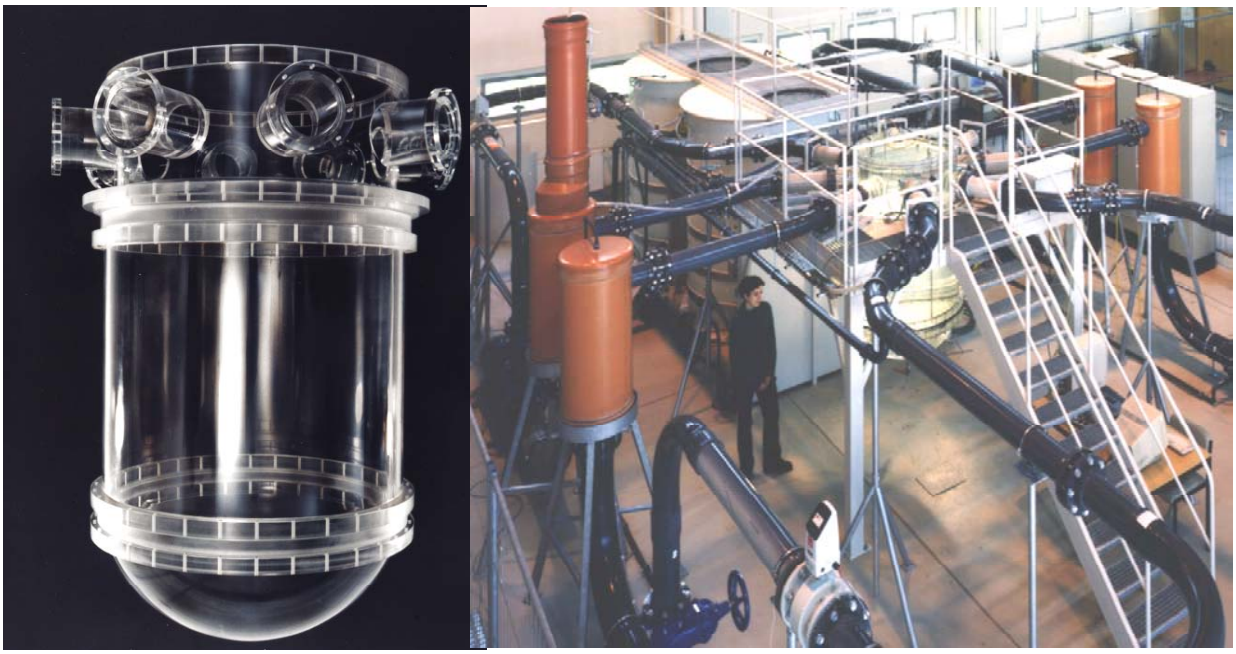

Fig. 1: Acryl model of the RPV and view on the test facility ROCOM

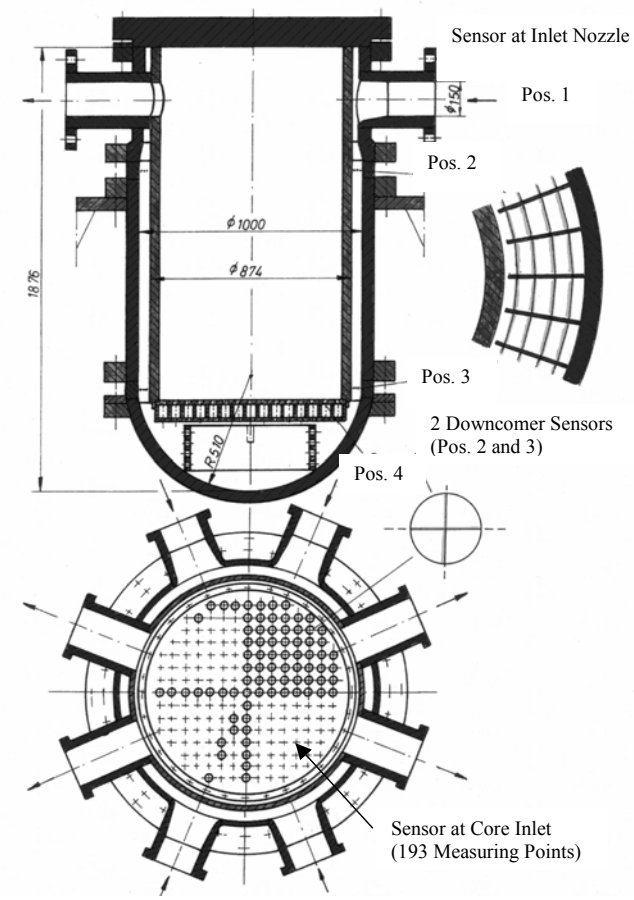

Fig. 2: Positions of wire mesh sensors in ROCOM

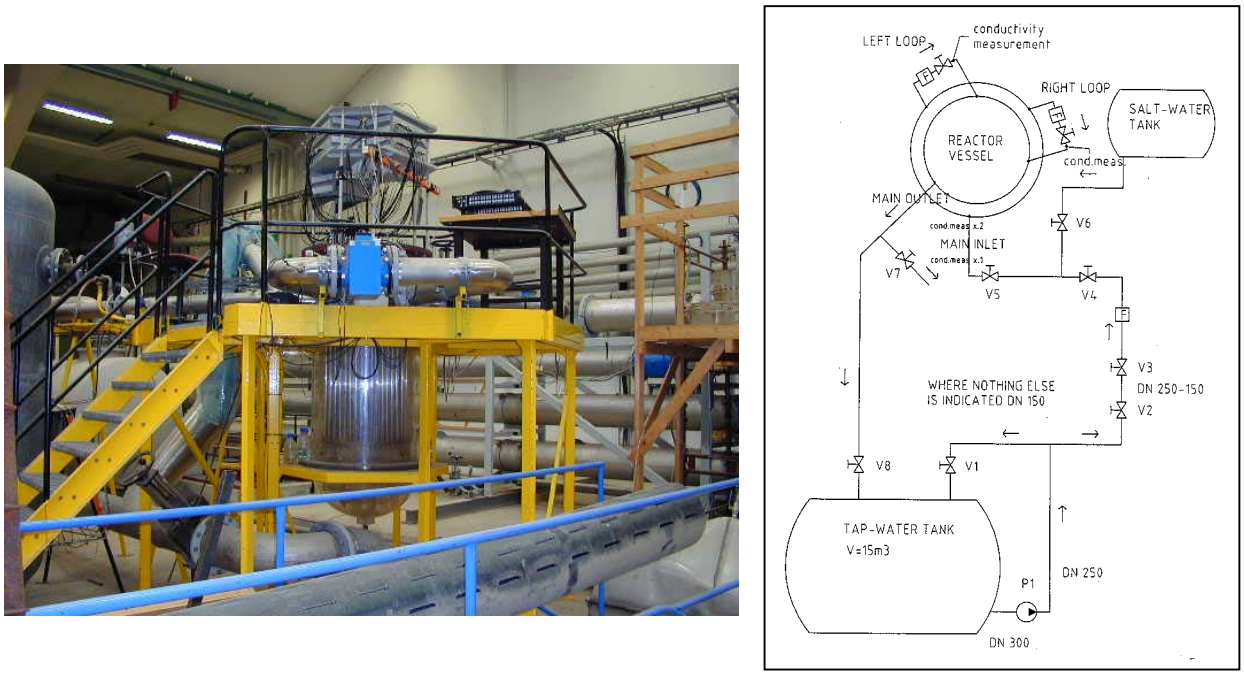

Fig.3: General view (left) and technological scheme (right) of the Vattenfall test facility

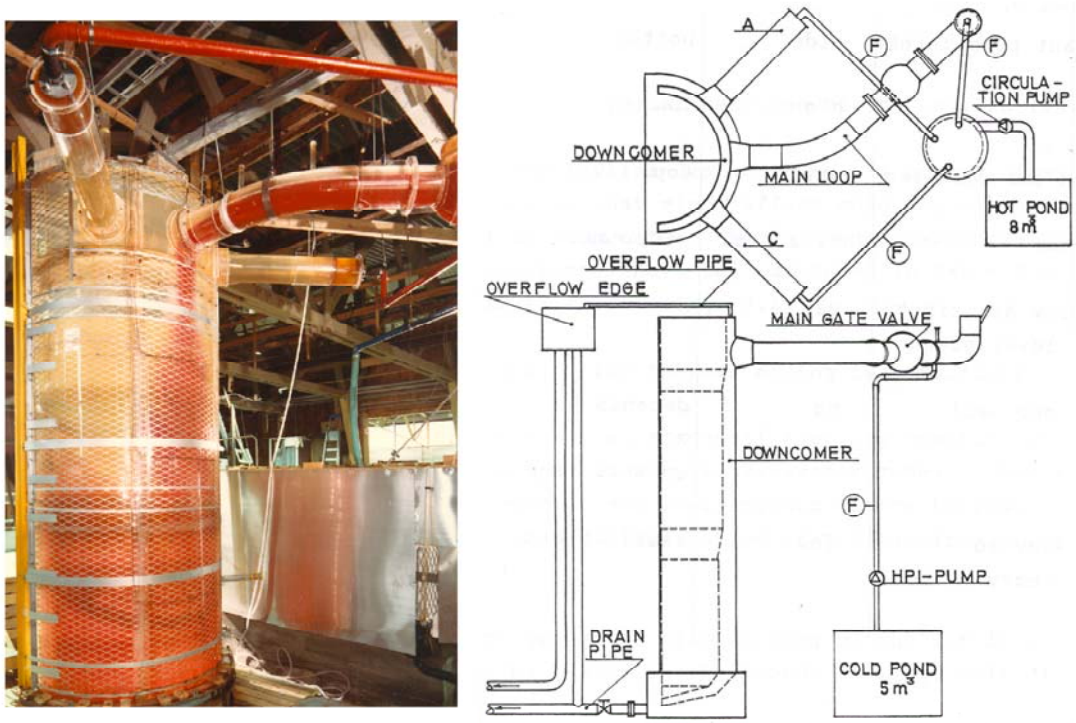

Fig. 4: General view, top view and side view of the Fortum PTS test facility

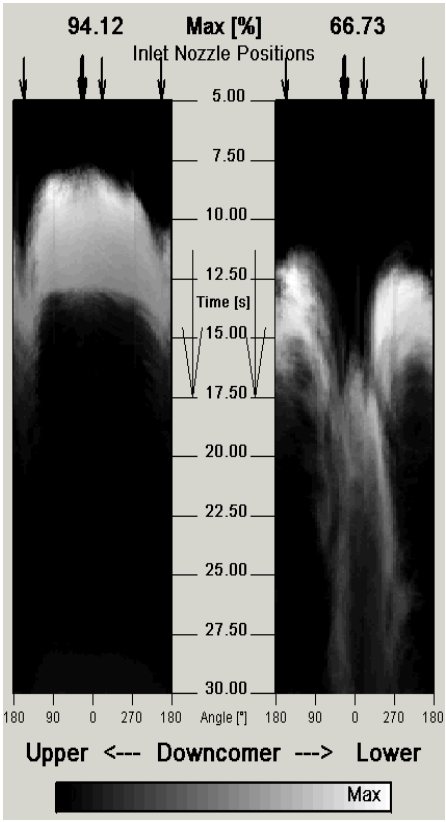

Fig. 5: Evolution of the mixing scalar distribution in the downcomer

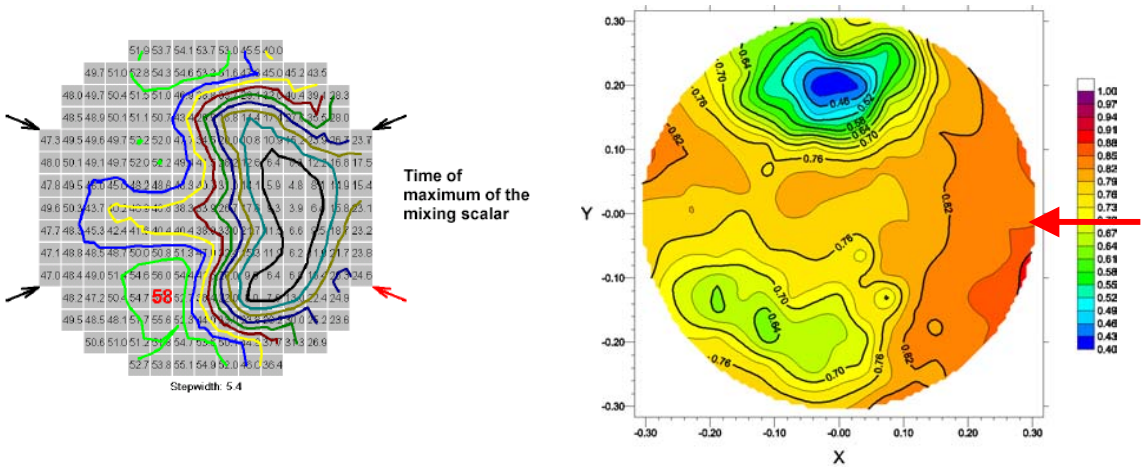

Red arrow – position of slug injection loop

Fig. 6: Mixing scalar distribution resp.
dimensionless boron concentration in the core inlet plane during pump start-up for the slug mixing tests ROCOM-02 (left) andVATT-02 (right)

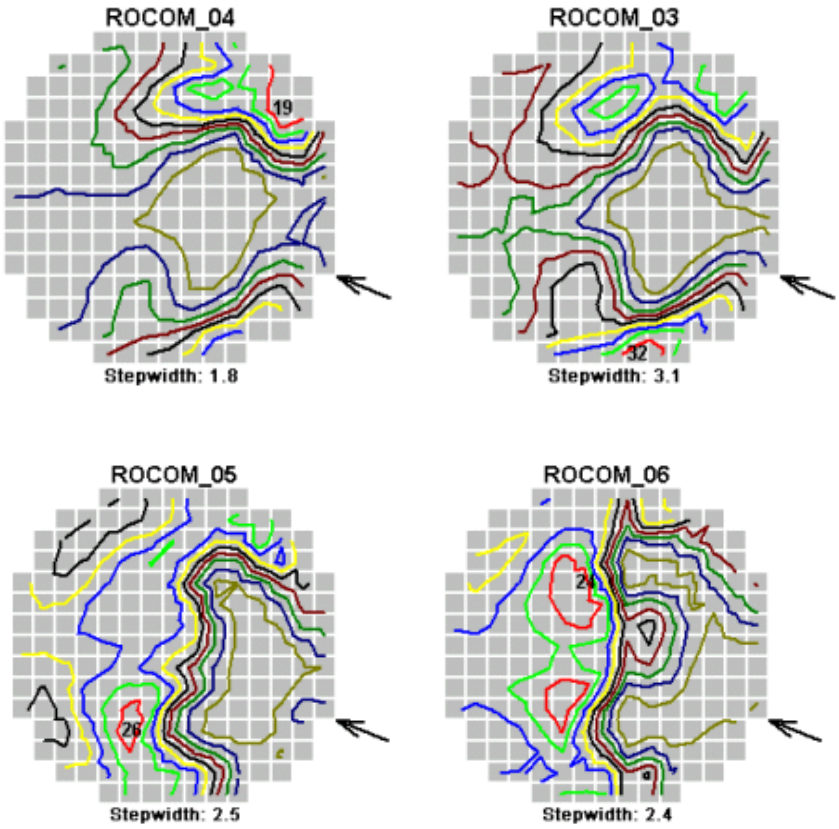

Fig. 7 Core inlet distribution of the mixing scalar at the time point of maximum in the experiments with variation of the initial slug position

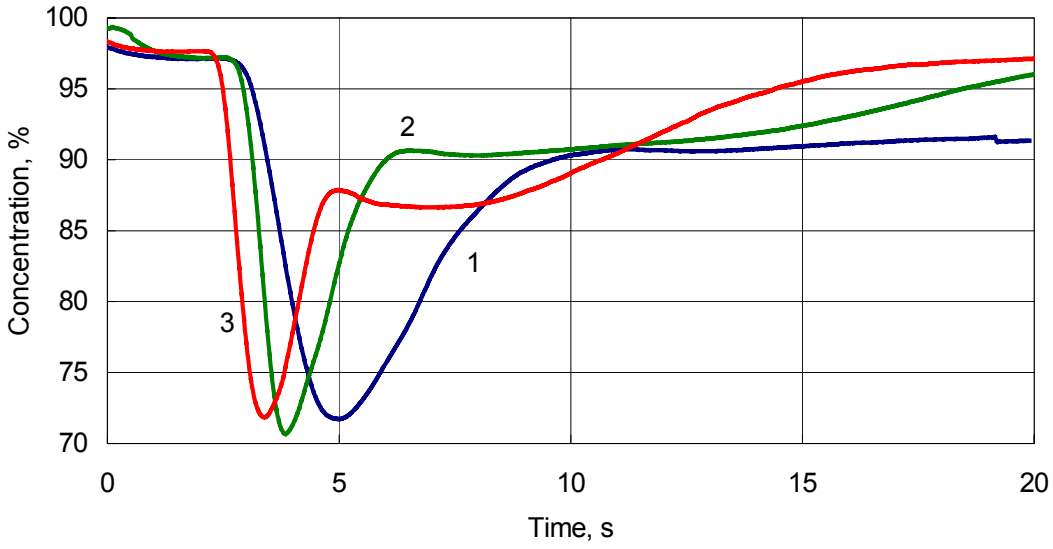

Fig. 8: Relative temperature averaged over the core inlet plane for the VVER-1000 mixing tests (1 - 175 m³/h, 2 - 470 m³/h, 3 - 815 m³/h)

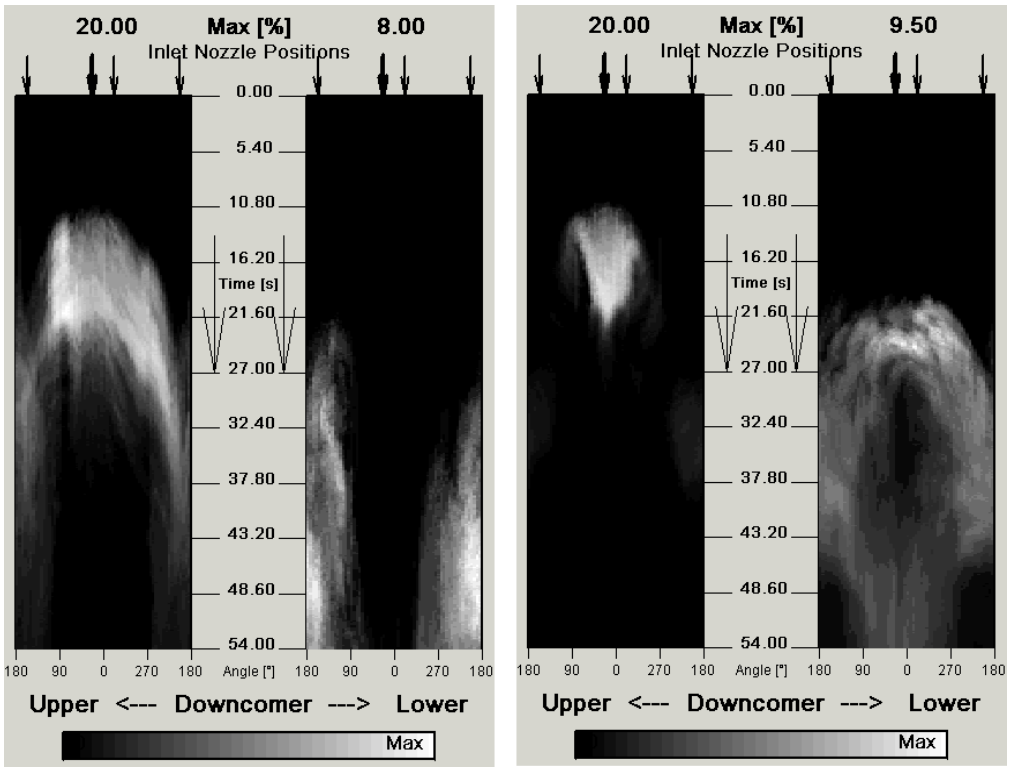

Fig. 9: Mixing scalar evolution in the downcomer in ROCOM buoyancy driven mixing tests (10 % mass flow rate, left – no density difference, right - 10 % density difference)

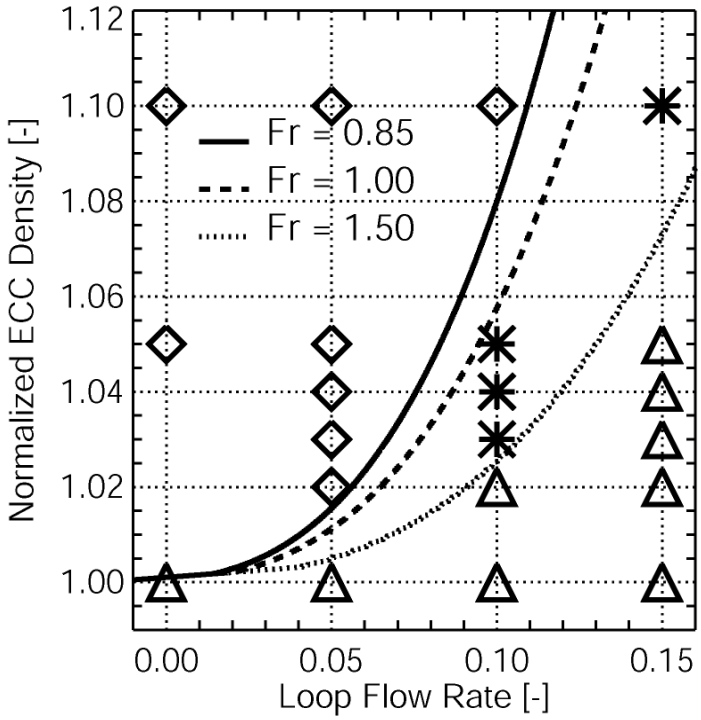

Fig. 10: Classification of the ROCOM tests with density differences with respect to the downcomer Froude number (equ. 2)

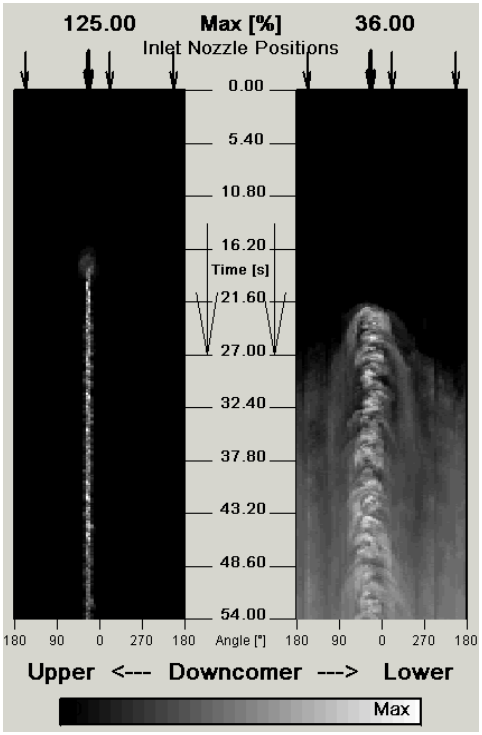

Fig. 11: Mixing scalar evolution in the downcomer in the ROCOM buoyancy driven mixing test D10M00 (no cold leg flow rate, 10 % density difference)

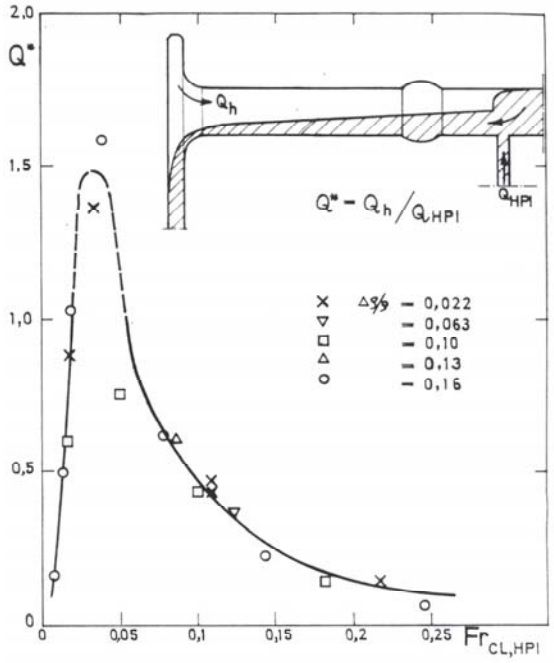

Fig. 12: Measured back flow ration in the Fortum PTS tests as a function of cold leg Froude number (equ. 3)

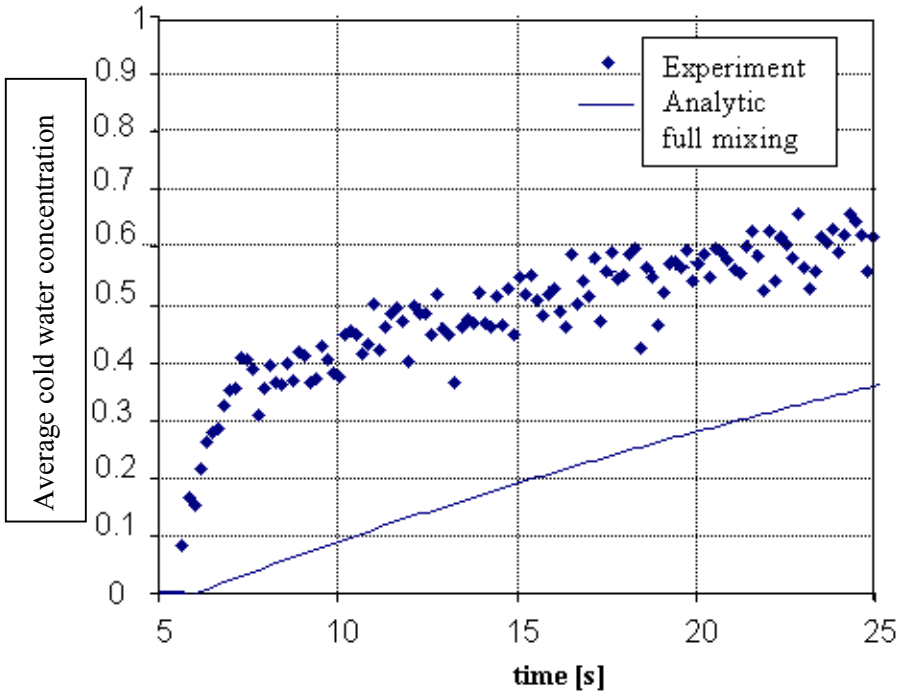

Fig. 13: Average HPI water concentration at axial level z= -164 mm below the middle of cold leg in Fortum PTS test #10

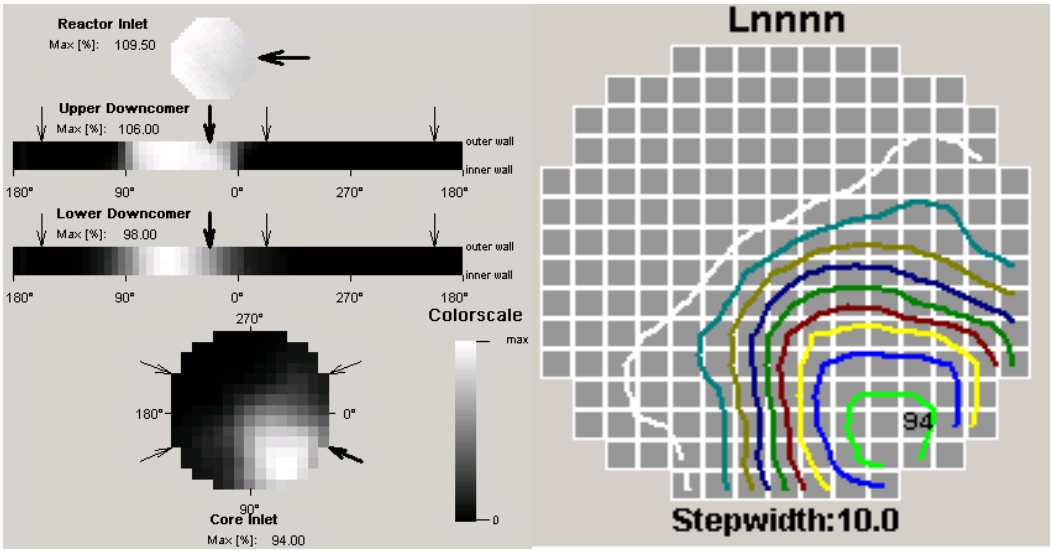

Fig. 14: Plateau-averaged mixing scalar in experiment ROCOM-stat01

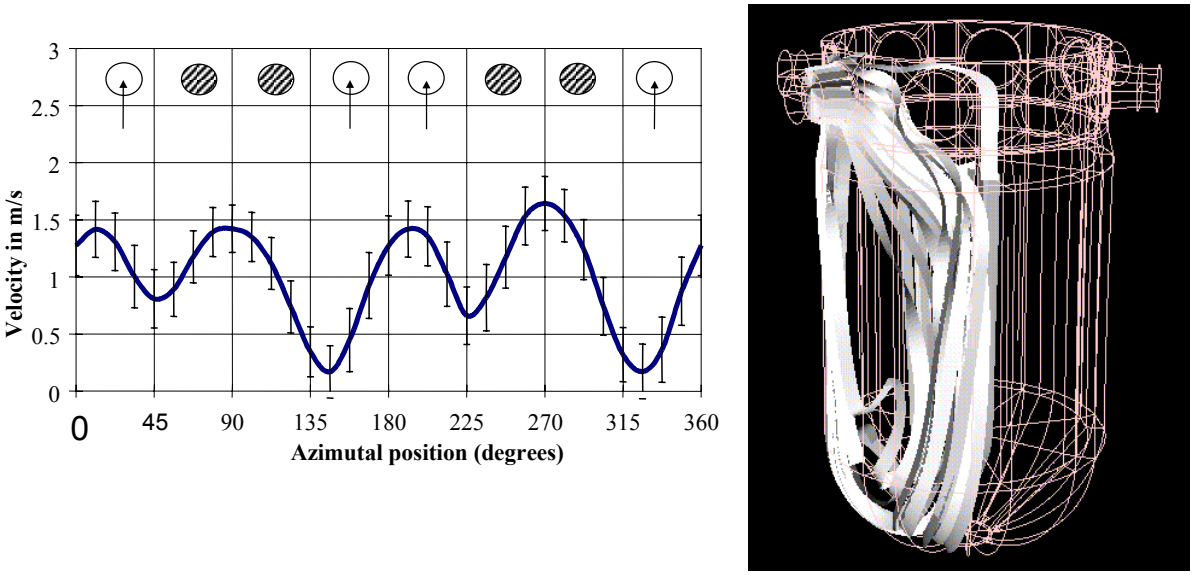

Fig. 15: Velocity distribution in the downcomer under normal operating conditions – measured vertical velocity component (left) and streamlines (right)

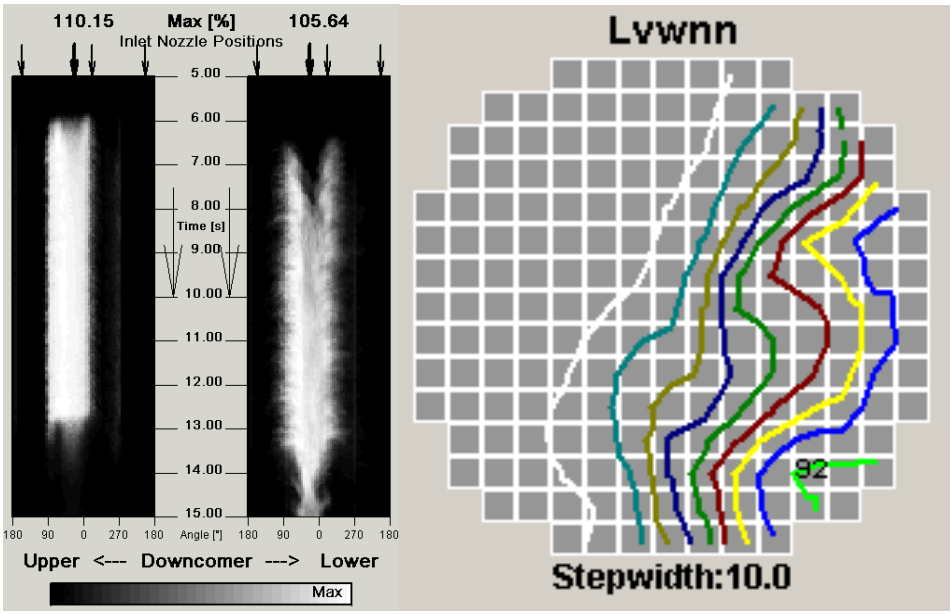

Fig. 16
Time evolution of the mixing scalar in the downcomer (left) and plateau-averaged mixing scalar at the core inlet (right) in experiment ROCOM-stat09 with asymmetric loop flow rates

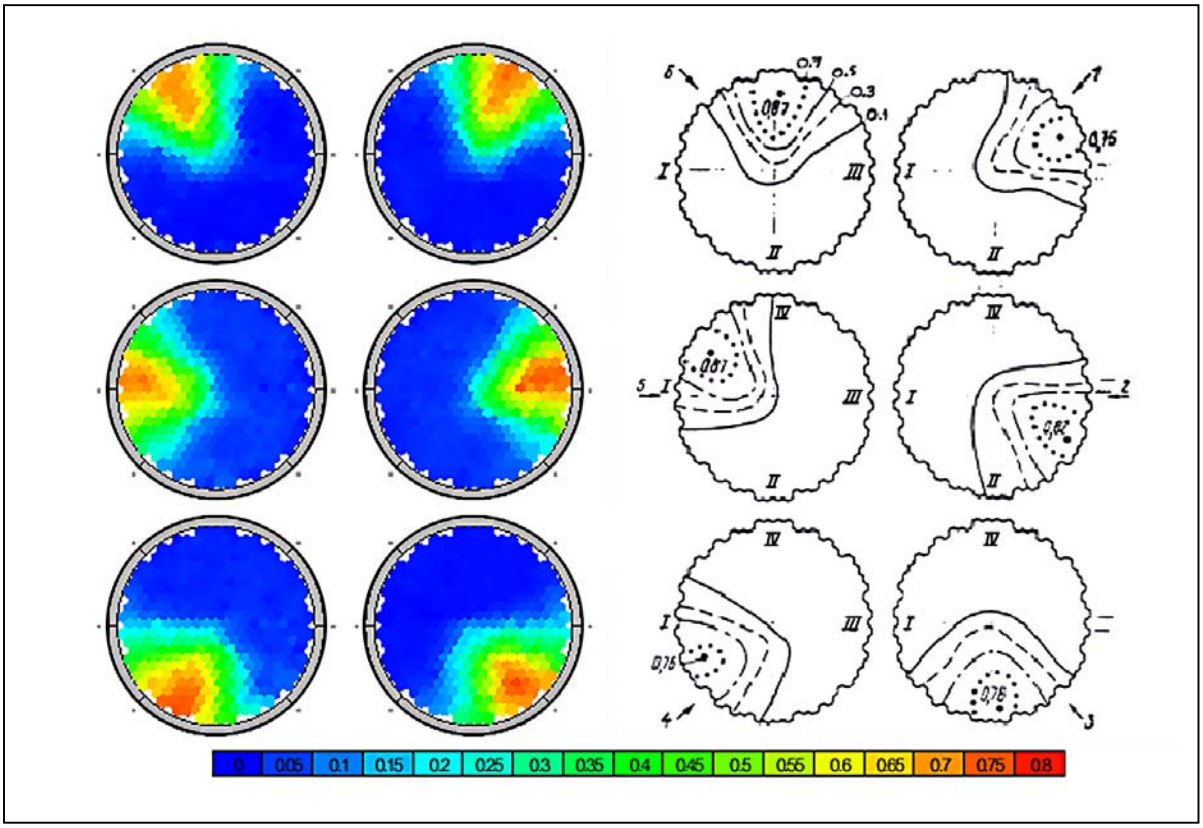

Fig. 17: By-loop mixing factors at Paks (upper) and Loviisa (lower) reactors (Elter, 2002 and Tsimbalov, 1982)

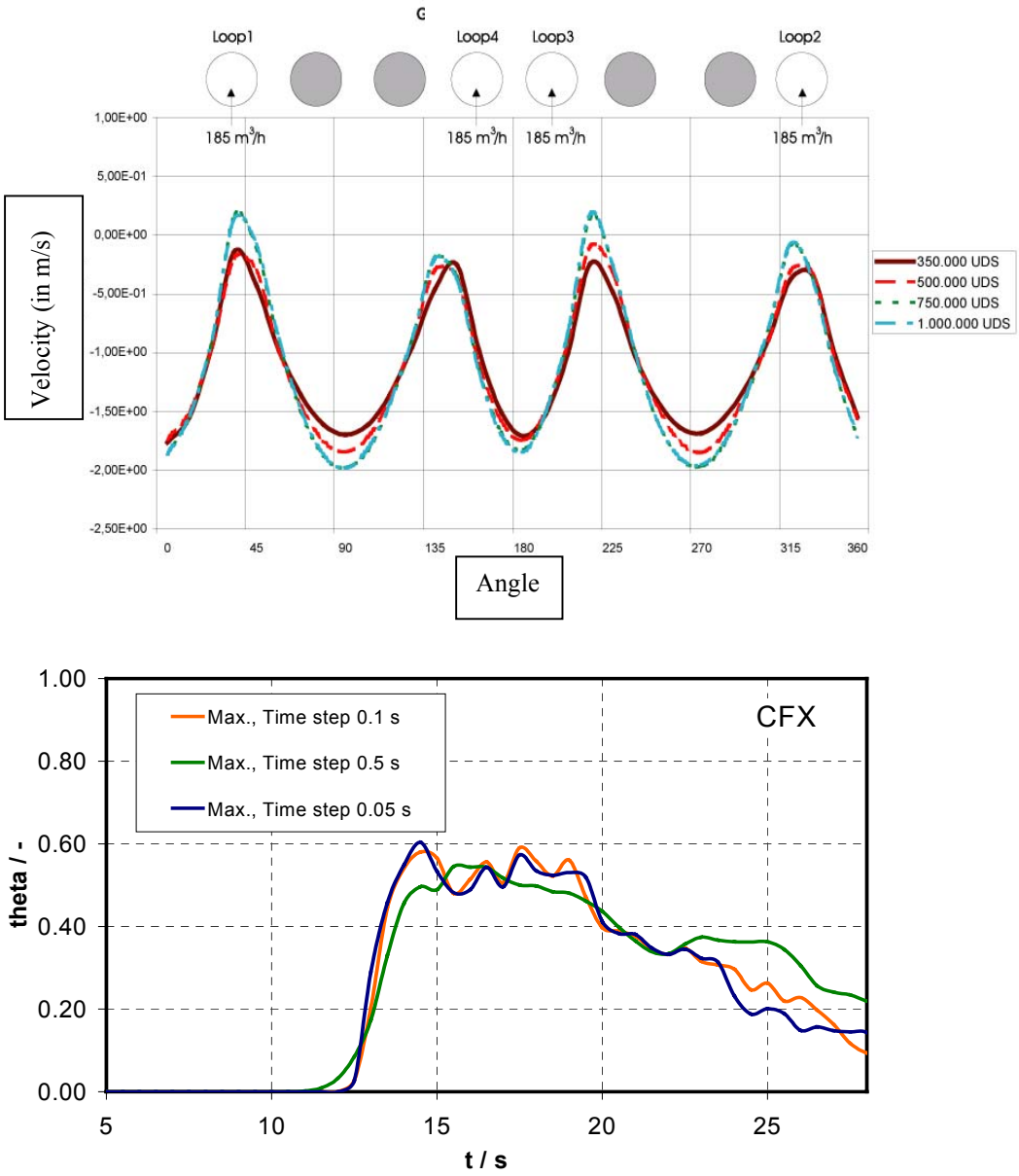

Fig. 18:
Mesh and time step refinement to obtain converged numerical solutions - velocity distribution in the downcomer (upper) and time dependent global maximum of the mixing scalar at the core inlet (lower)

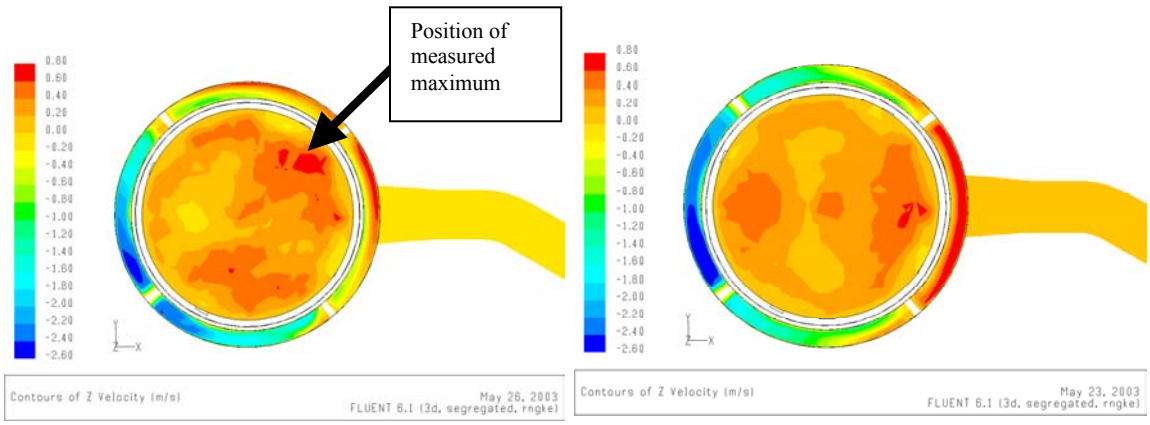

Fig. 19: Calculated velocity distribution in the core inlet plane at the – second order (left) and first order (right) solution

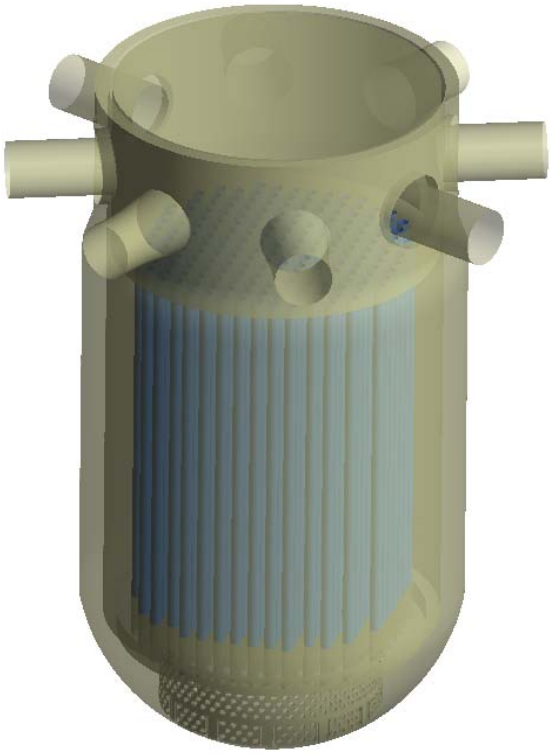

Fig. 20: Visualisation of the ROCOM production mesh for the CFX-5 calculations

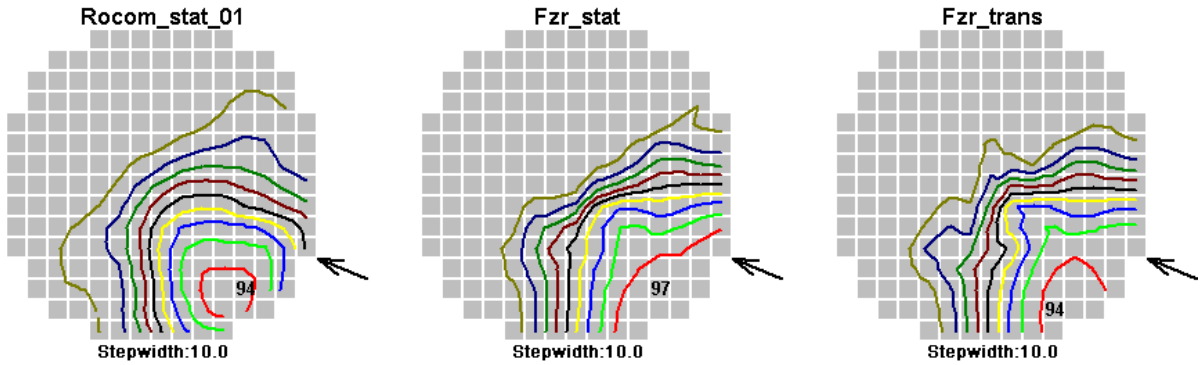

Fig. 21: Comparison of results from a steady-state and a transient CFX calculation for the test ROCOM-stat01

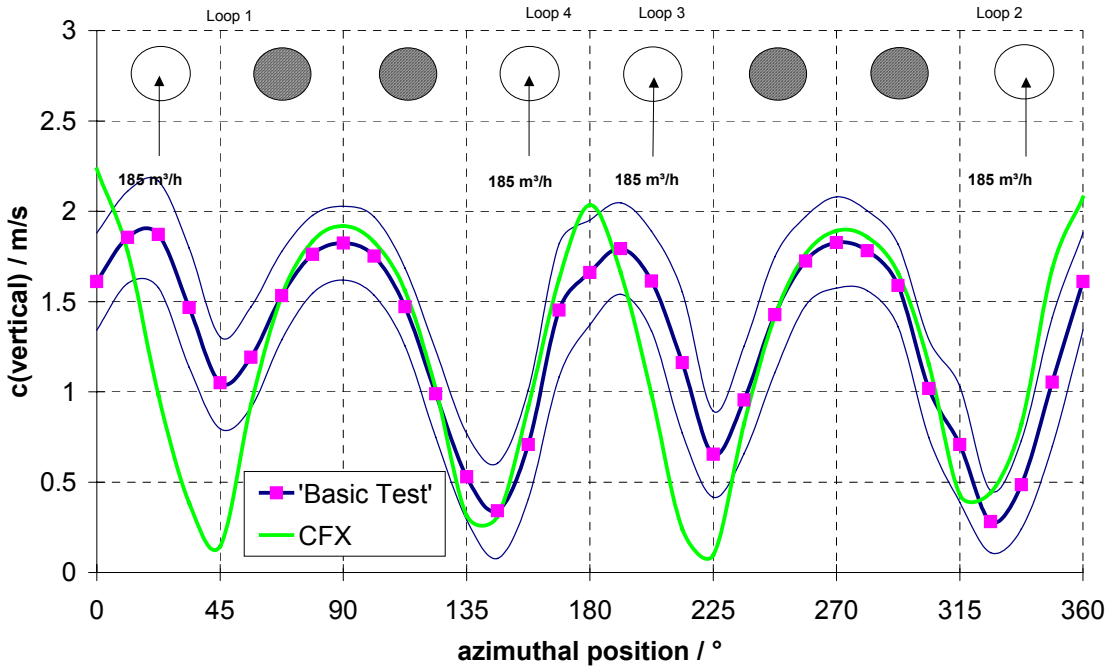

Fig. 22: Velocity measurements vs. CFX-4 results at the end of the downcomer

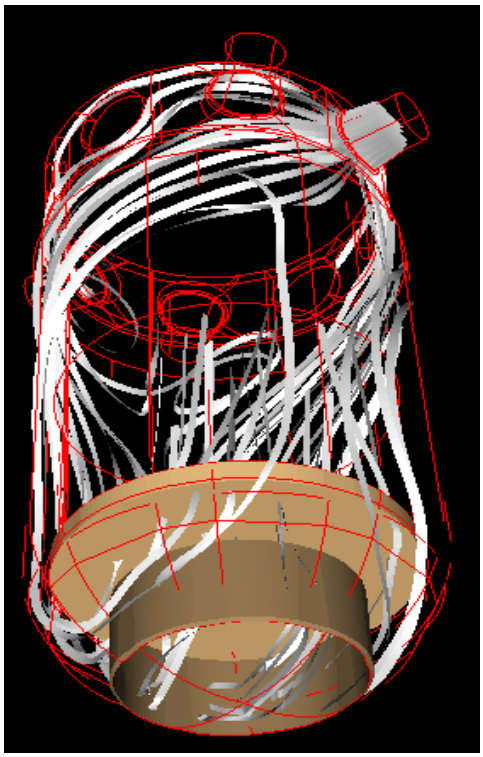

Fig. 23: Flow picture (stream lines) at 15 s after the start-up

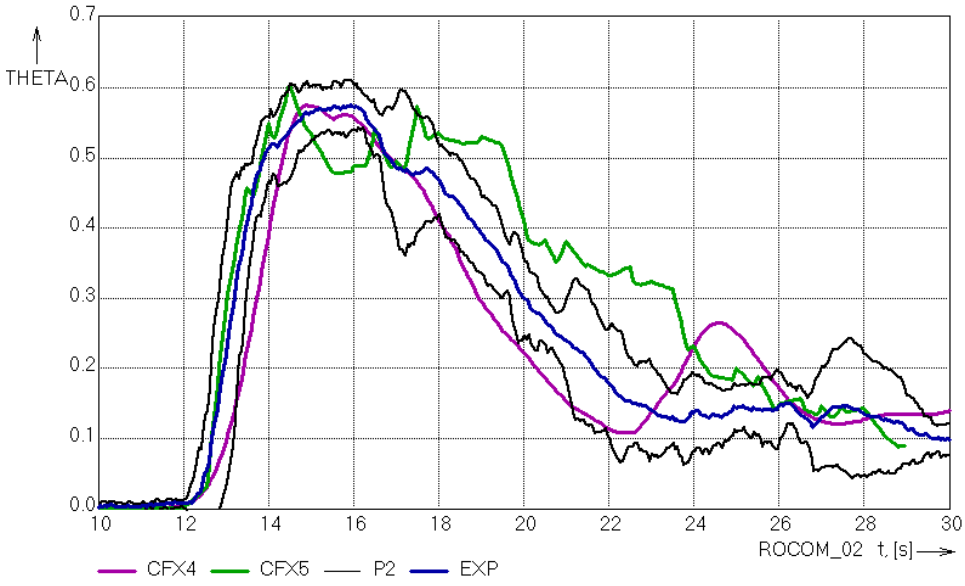

Fig. 24: Comparison of maximum mixing scalar between measurement and CFD calculations for the experiment ROCOM-02

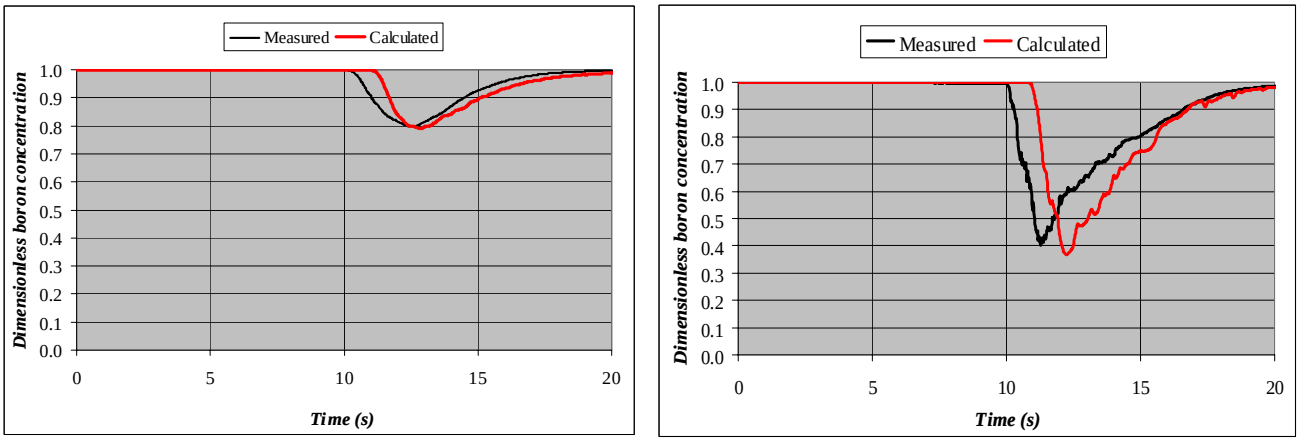

Fig. 25:
VATT-02 slug mixing transient. Mean dimensionless boron concentration (left) and minimum relative boron concentration at core inlet (independently of position) as a function of time

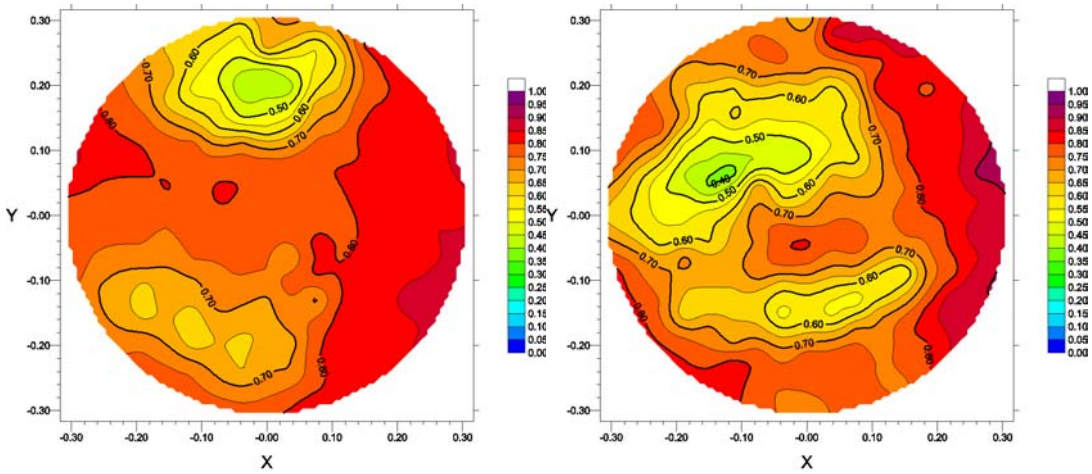

Fig.26
VATT-02 slug mixing transient. Minimum relative boron concentration, independently of time. Measurement to the left, CFD calculation to the right

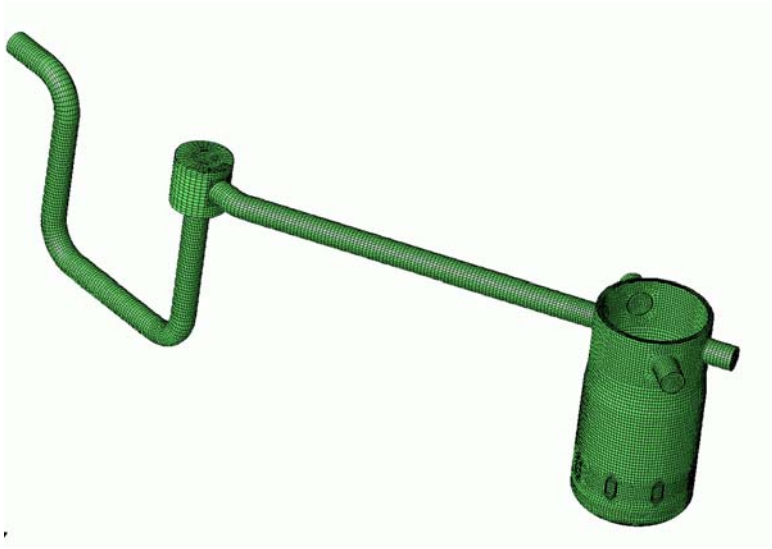

Fig. 27: Computational domain with grid used in Gidropress test No.1– overall view

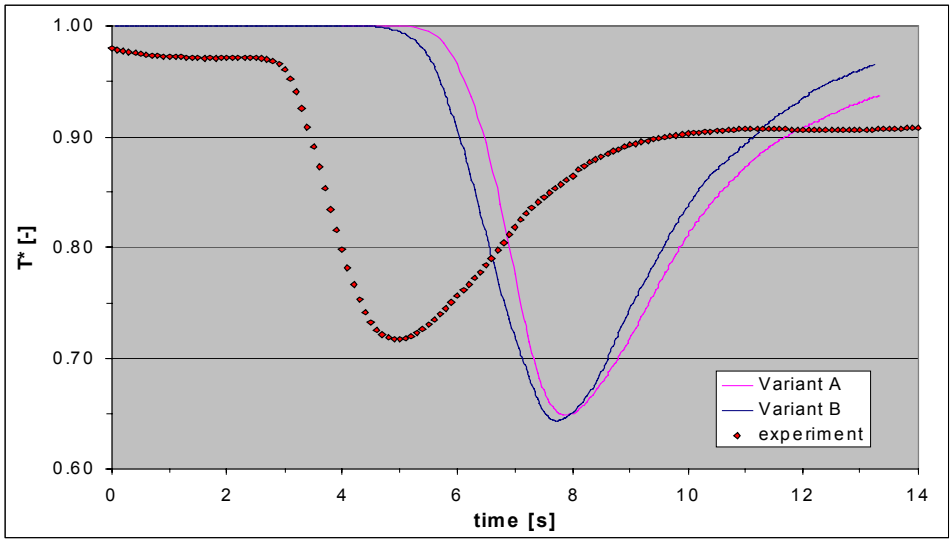

Fig. 28: Test 1 - Average dimensionless temperature at the core inlet vs. time

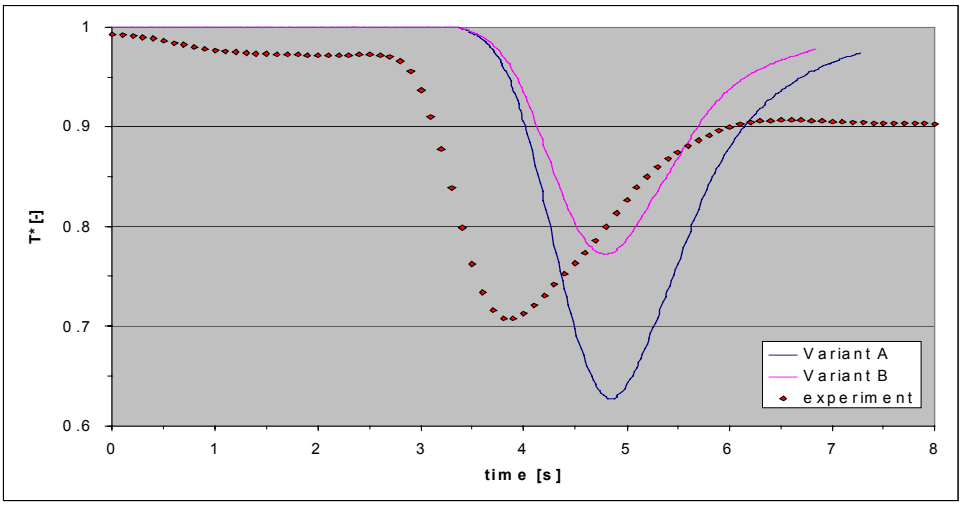

Fig. 29: Dimensionless average core inlet temperature for variant 2A with zero wall heat fluxes and variant 2B with constant wall temperature

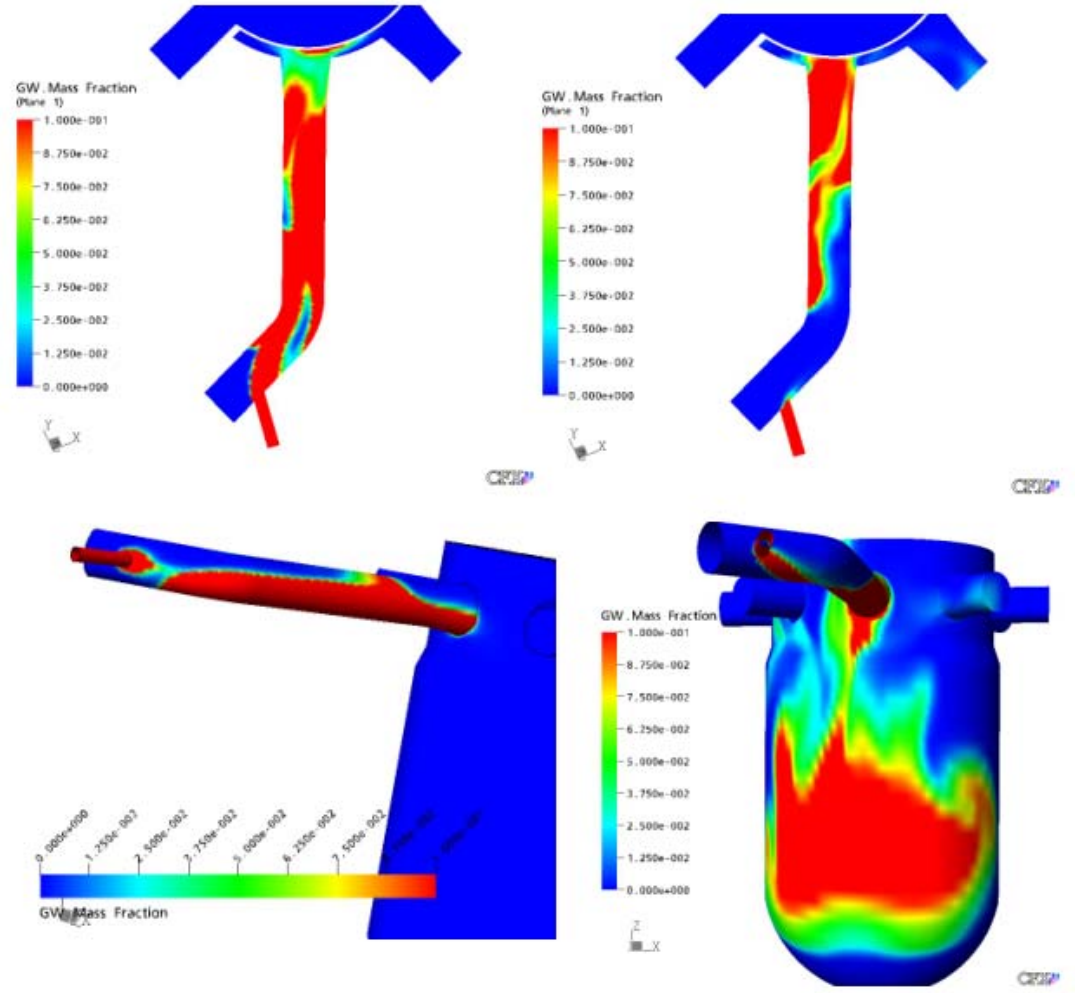

Figure 30: Glucose concentration in cold leg (upper) and downcomer (lower)
left: t= 10 s, right: t = 20 s

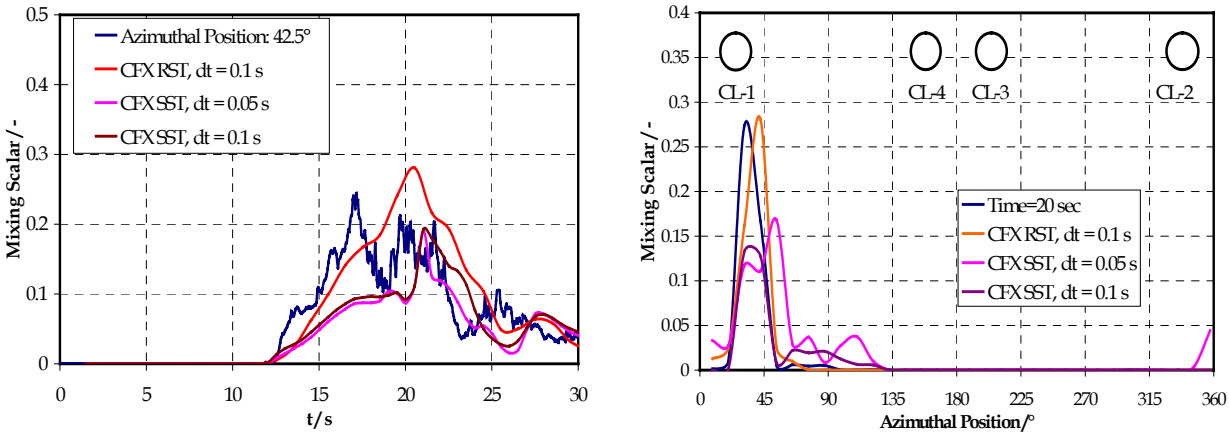

Fig. 31: Mixing scalar at local position and circumferential distribution in the upper downcomer for the experiment D10M05

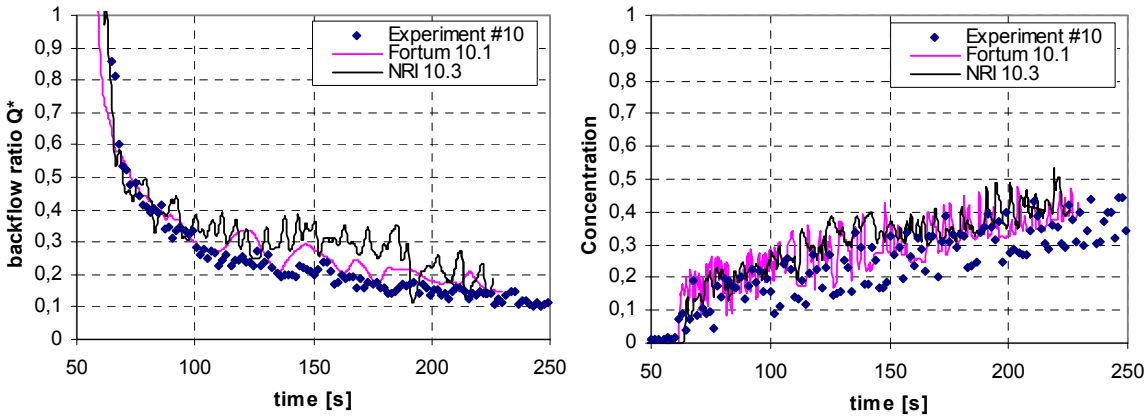

Fig. 32: Backflow ratio (left) and cold HPI water concentration at pressure vessel wall at level z = -1460 (right) during simulations of experiment #10

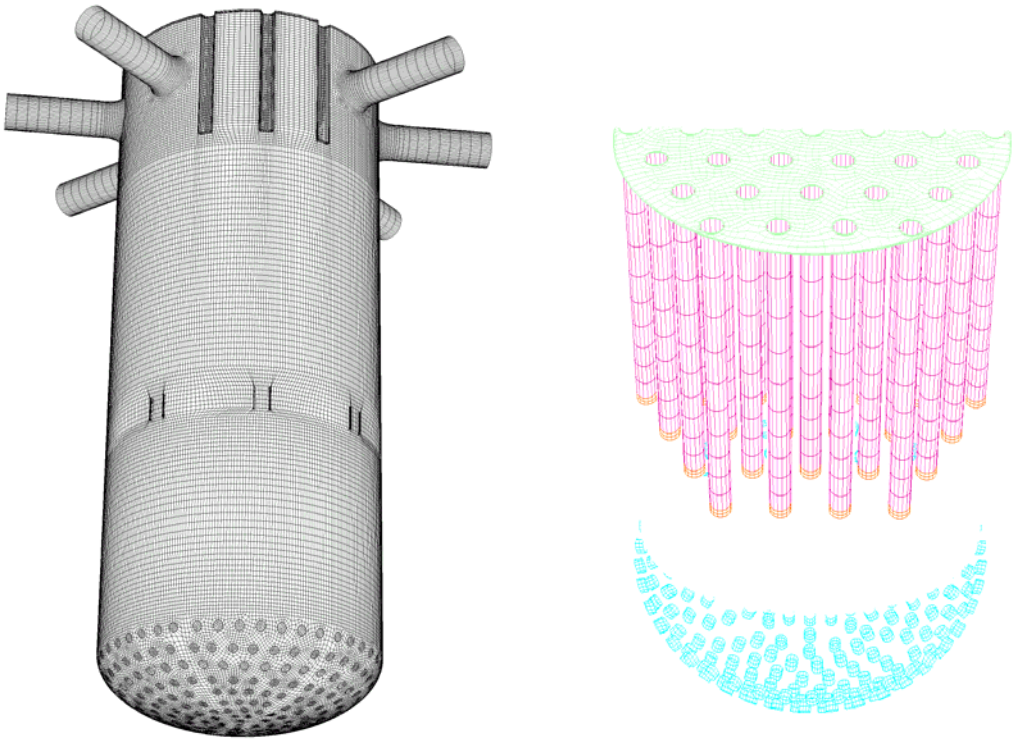

Fig. 33: VUJE model of VVER 440 V-213 reactor (left) and reactor internals (right)

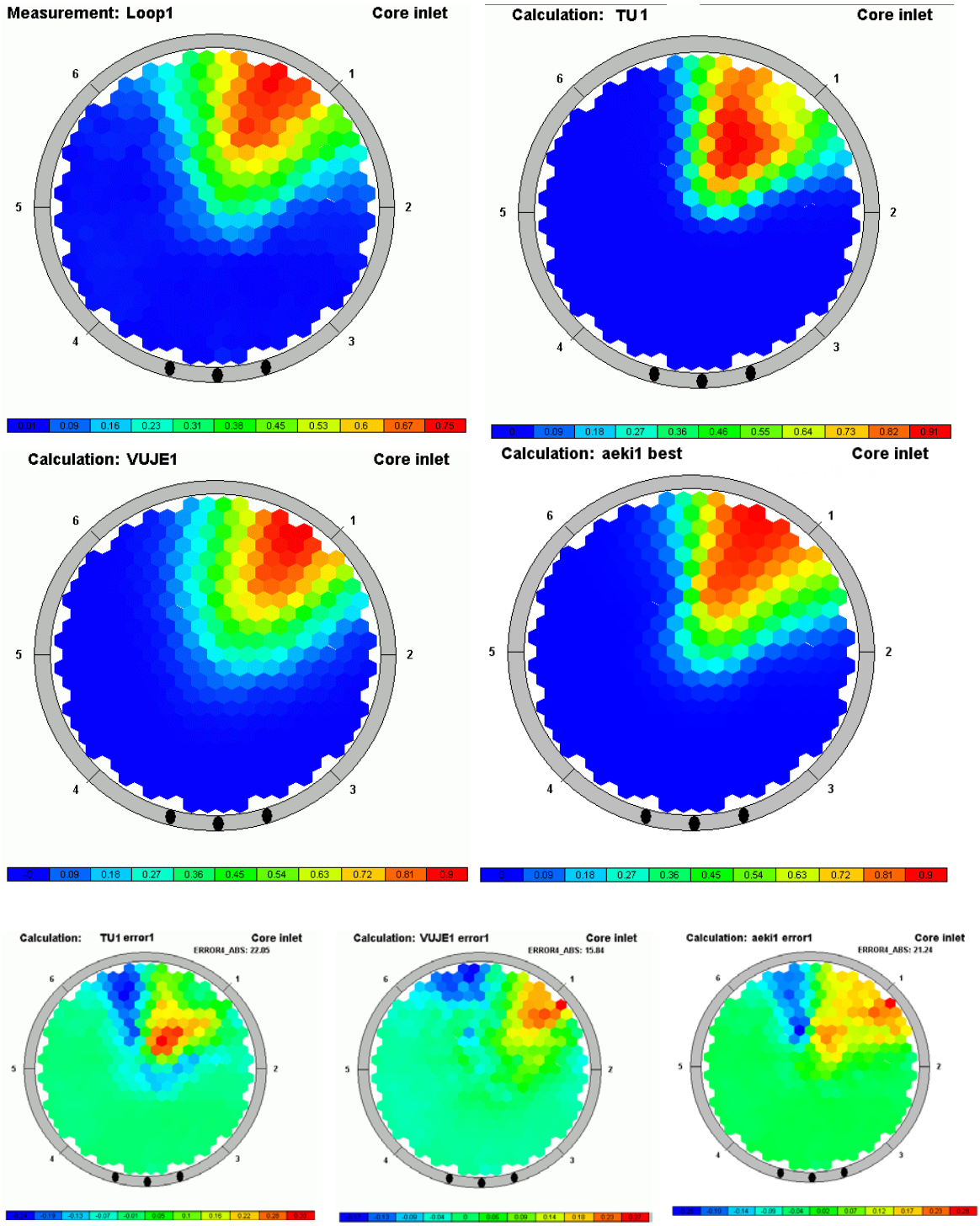

Fig. 34
Comparison of calculated core inlet temperatures with measured data for loop one (upper) and deviations from measurement (lower)